University of South Carolina

Image-based Measurements in Solid Mechanics: A Brief History, Static and Dynamic Application Examples and Recent Developments

Michael A. Sutton, PhD
Carolina Distinguished Professor
Department of Mechanical Engineering
University of South Carolina
Columbia, SC 29208

University of South Carolina

Outline

- **Brief History**
  - *Measurement Methods*
  - *Digital Image Correlation*
- **Digital Image Correlation Methods**
  - *2D-DIC*
    - *Early Applications*
  - *3D-DIC*
    - *Early Applications*
  - *V-DIC*
    - *Applications*
- **3D-DIC Applications and Details**
  - *Composite Materials in Bending-Compression*
  - *Shingles in 340 km/h winds*
- **The Future**
  - *Integration with Design and Development*
  - *Future Trends in Digital Image Based Methods*
- **Acknowledgements**
  - Sponsors and students who did the work

Brief History: Measurement Methods

- In the mid 20th century, experimental methods in solid mechanics focused on point-wise measurements for quantitative data

1

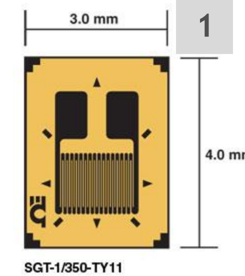

- Early full-field measurements were made in photo-elastic, polymeric materials
  - Through-thickness average effects
  - Local effects using a complex method known as "stress-freezing"

2

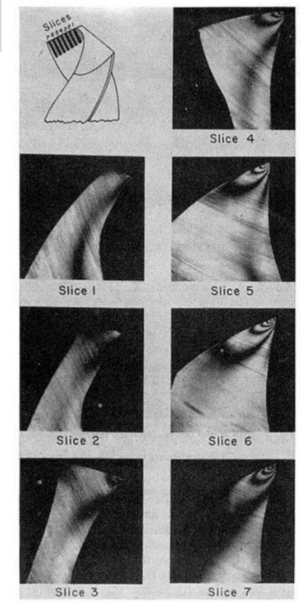

- The advent of lasers and interferometry methods circa 1960s provided investigators with new full-field measurement capability.
  - Recording was via film media

3

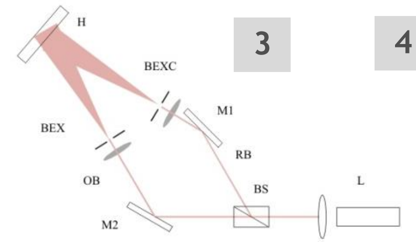

4

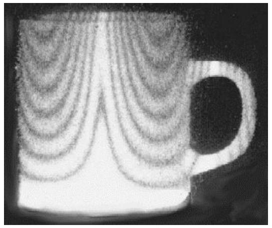

Brief History: Measurement Methods

- Vincent J. Parks, 1980
  - Experimentally showed that the range of displacement measurements that was possible using speckle photography was limited due to de-correlation.

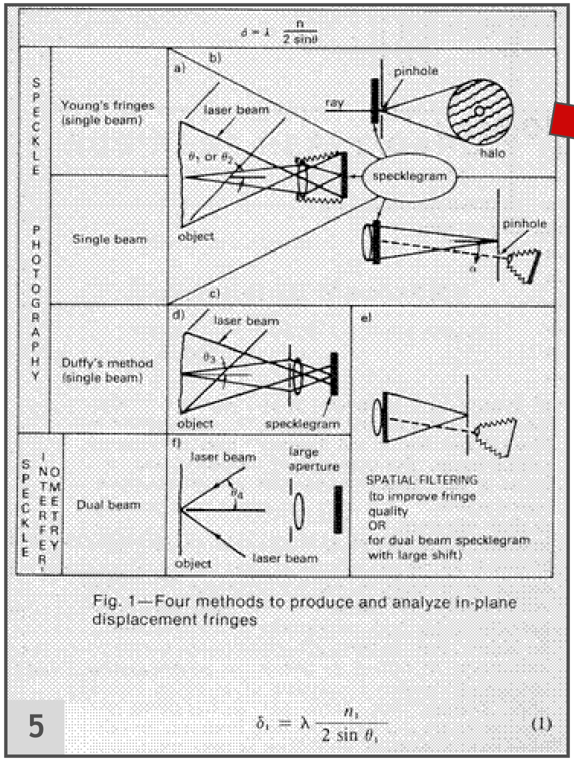

Fig. 1—Four methods to produce and analyze in-plane displacement fringes

$$\delta_1 = \lambda \frac{n_1}{2 \sin \theta_1} \quad (1)$$

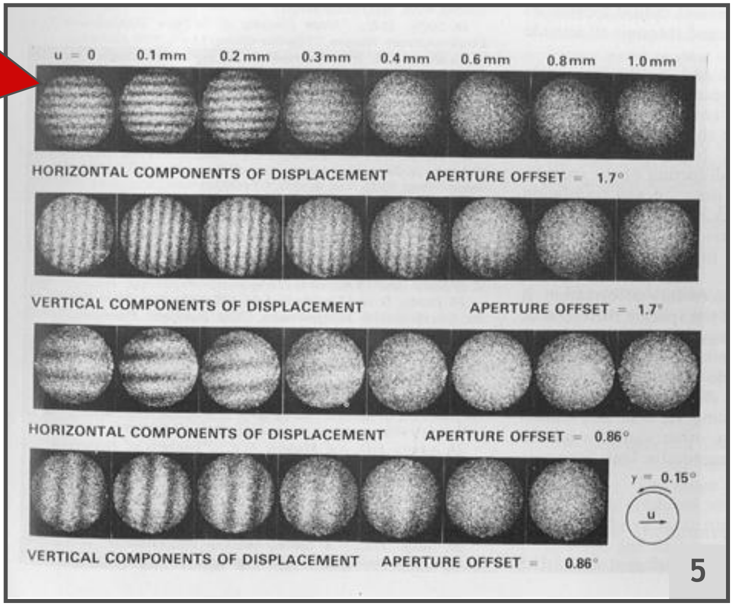

Brief History: Digital Image Correlation

- **1980, William F. Ranson and Walter H. Peters III**
  - For 2D, through-thickness averaged, ultra-sound applications, proposed approach for conversion of digitized ultra-sound images into estimates for local surface displacements by employing continuum-based matching principles
- **1982, Cheng and Sutton; Sutton and Wolters**
  - Developed non-linear least squares approaches using first-order gradients in a matching function to obtain local displacements.
- **1985, TC Chu et al**
  - Using a DAGE MTI analog camera to record images of a speckle pattern at 8 bits, demonstrating conclusively that the method could be used to measure deformations
    - Translations, large or small
    - Rotations, large or small
    - Strains, large and relatively small

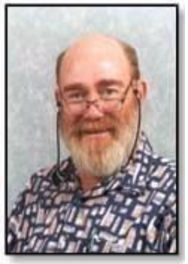

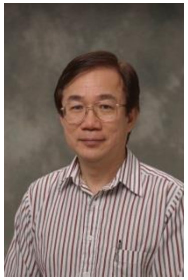

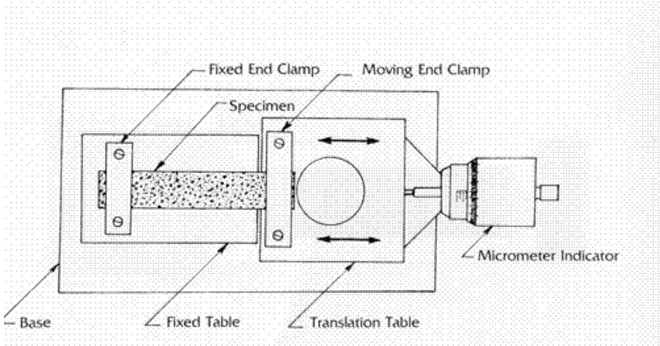

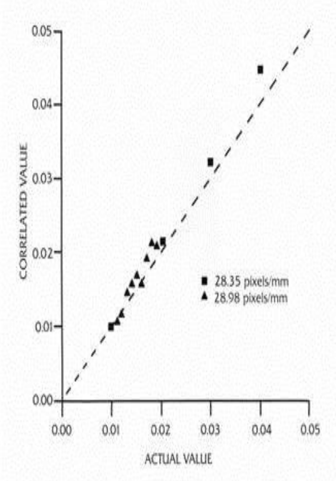

Figure 24
Correlated Data for Finite Strain Test

Brief History: Digital Image Correlation

University of South Carolina

- **1989, Bruck et al**
  - Developed and demonstrated order of magnitude speed improvement using Hessian-based methodology for computing iterative improvements in optimal matching positions of subsets
  - Used linear shape functions for subset-based matching
- **1993, Luo, Chao et al**
  - Developed a stereo-vision system and verified the ability to make local strain and deformation measurements in cracked material
- **1996, Helm, McNeill et al**
  - Developed a robust stereo-vision system and demonstrated used on full-scale aero-structures as well as on laboratory-scale specimens
- **2000, Bay et al**
  - Extended 2D and 3D methods to volumetric images and performs digital image correlation on volumetric elements on the interior of a material
  - Limited to those materials providing sufficient contrast during tomographic imaging
  - Requires a tomographic imaging facility






Brief History: Digital Image Correlation

- The rapid growth of **computer technology** that spurred continued growth of computational methods also provided the foundation for the explosion of growth in vision-based full-field experimental measurement method
    - 2D-DIC for SEM, AFM and planar loading and surfaces
    - 3D-DIC for general motion and deformation of curved or planar surfaces
    - V-DIC or Digital Volume Correlation for interior deformation measurements in opaque solids
- Today, the methods are used worldwide by scientists and investigators seeking to obtain full-field quantitative measurement of motions and deformations.

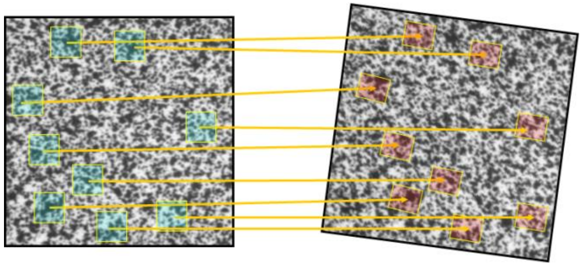

12, 13

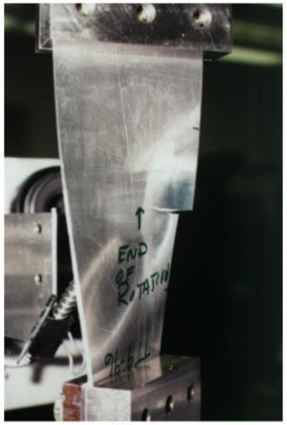

- X-Radia Micro-CT

14

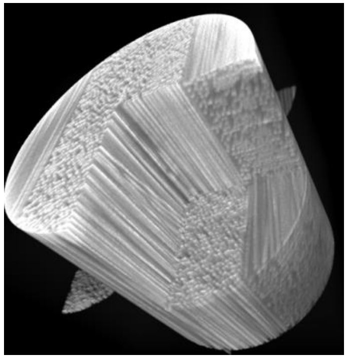

2D Image Correlation: Basic Concepts

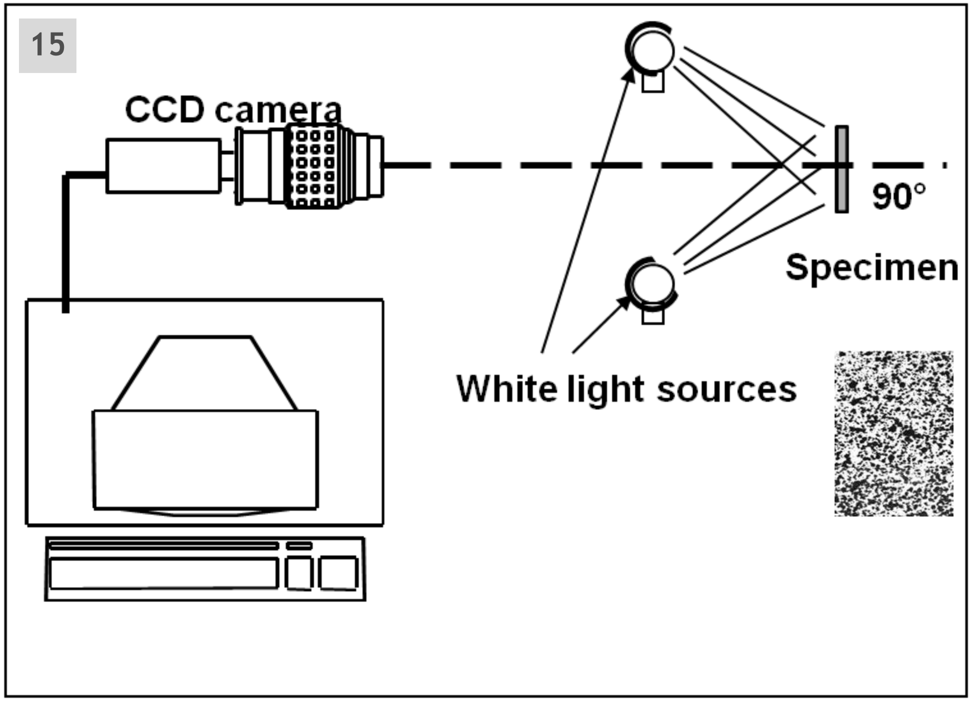

Single CCD camera positioned perpendicular to object surface.

- Specimen has a random pattern on its surface
- Uniform illumination is provided by white light sources
- Loading nominally in-plane, minimizing out of plane motion

2D Image Correlation: Basic Concepts

General Remarks

- Relatively simple to use under both laboratory and field conditions
- Relatively simple pattern application for many applications
  - Not so simple for microscale applications
- Data acquisition and data analysis procedures are well established
- Successfully used to make measurements on a range of specimen sizes from 0.01 mm to 2m
- Near real time analysis, with data analyzed at > 15000 subsets per second
- Accuracy nominally unaffected by large in-plane rotations or translations
  - Strain levels over 300% have been successfully measured
- Variability less than 0.01 pixels in displacement on a point-to-point basis are commonly obtained
- Accuracy of 100 μs or smaller in strain on a point-to-point basis through differentiation of smoothed displacement data.
- Effect of out-of-plane displacement is readily estimated and minimized using equation w/Z, where w is out-of-plane motion and Z is distance from specimen to camera

2D Image Correlation: Key Developments

- First LEFM measurements with DIC (1985-1987)

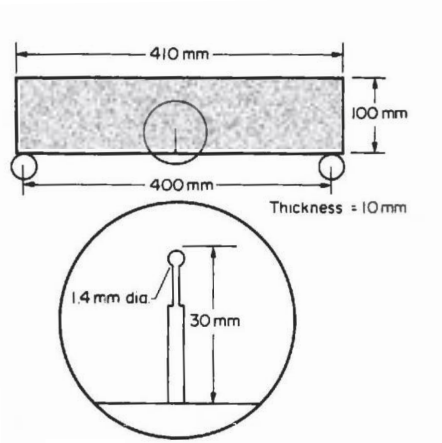

3-Point bend specimen.

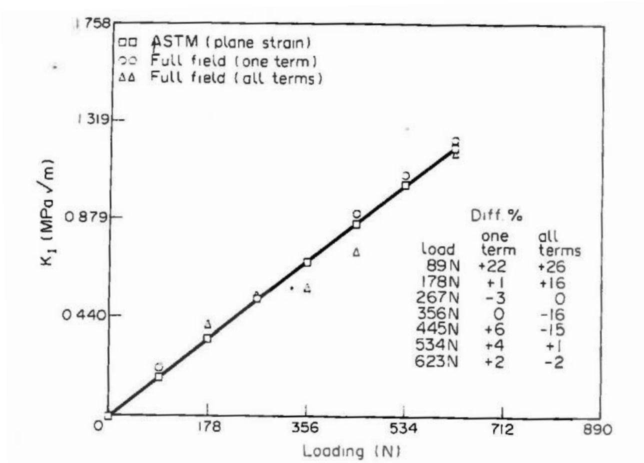

- Improving and speeding up DIC; differential corrections for efficient DIC (1987-1989)

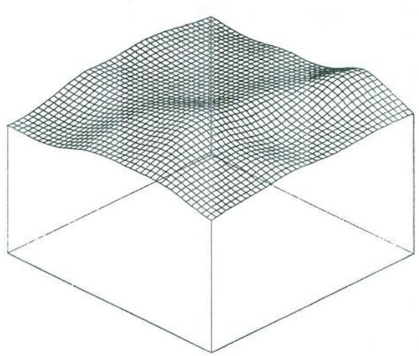

$$S\left(x, y, u, v, \frac{\partial u}{\partial x}, \frac{\partial u}{\partial y}, \frac{\partial v}{\partial x}, \frac{\partial v}{\partial y}\right) = 1 - \frac{\Sigma\,[F(x,y) * G(x^*, y^*)]}{[\Sigma\,(F(x,y)^2) * \Sigma(G(x^*,y^*)^2)]^{1/2}}$$

$$x^* = x + u + \frac{\partial u}{\partial x}\Delta x + \frac{\partial u}{\partial y}\Delta y$$

$$y^* = y + v + \frac{\partial v}{\partial x}\Delta x + \frac{\partial v}{\partial y}\Delta y$$

$$P_i = \begin{Bmatrix} u \\ v \\ \frac{\partial u}{\partial x} \\ \frac{\partial u}{\partial y} \\ \frac{\partial v}{\partial x} \\ \frac{\partial v}{\partial y} \end{Bmatrix} \qquad \nabla(P_i) = \begin{pmatrix} \frac{\partial S}{\partial u} \\ \frac{\partial S}{\partial v} \\ \frac{\partial S}{\partial\left(\frac{\partial u}{\partial x}\right)} \\ \frac{\partial S}{\partial\left(\frac{\partial u}{\partial y}\right)} \\ \frac{\partial S}{\partial\left(\frac{\partial v}{\partial x}\right)} \\ \frac{\partial S}{\partial\left(\frac{\partial v}{\partial y}\right)} \end{pmatrix}$$

$H_{ij} = [\partial^2 S / \partial P_i \partial P_j]$

$$\Delta P_i = -H^{-1}(P_i) * \nabla(P_i)$$

TABLE 1—AVERAGE CPU TIME* (IN SECONDS) per subset

Test Performed	Bicubic 50 × 50 Subsets	Bicubic 20 × 20 Subsets	Column 50 × 50 Subsets	Column 20 × 20 Subsets
Translation	20.72	5.95	54.21	8.28
Rotation	55.36	6.63	n/a	n/a

*For a Vax 11/780 minicomputer

2D Image Correlation: Key Developments

- First high temperature measurements with DIC (1994-1996)

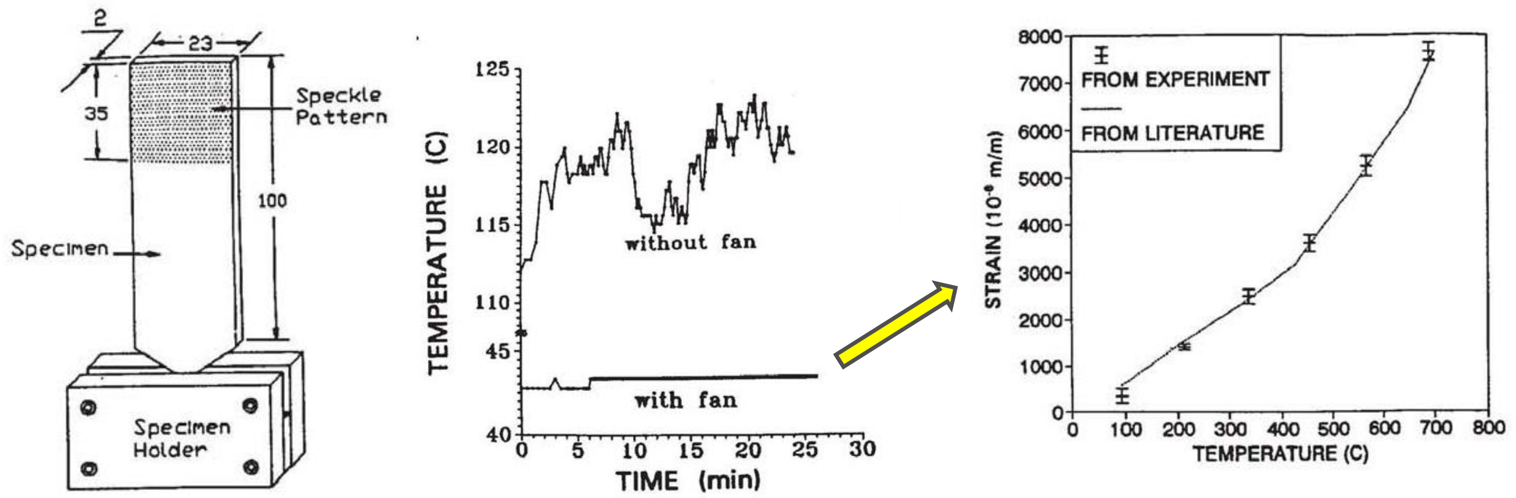

- First long-duration creep fracture w/DIC measurements. IN800 at 650°C for 147 hrs in lab air. Ceramic paint and pattern (1995-1998).

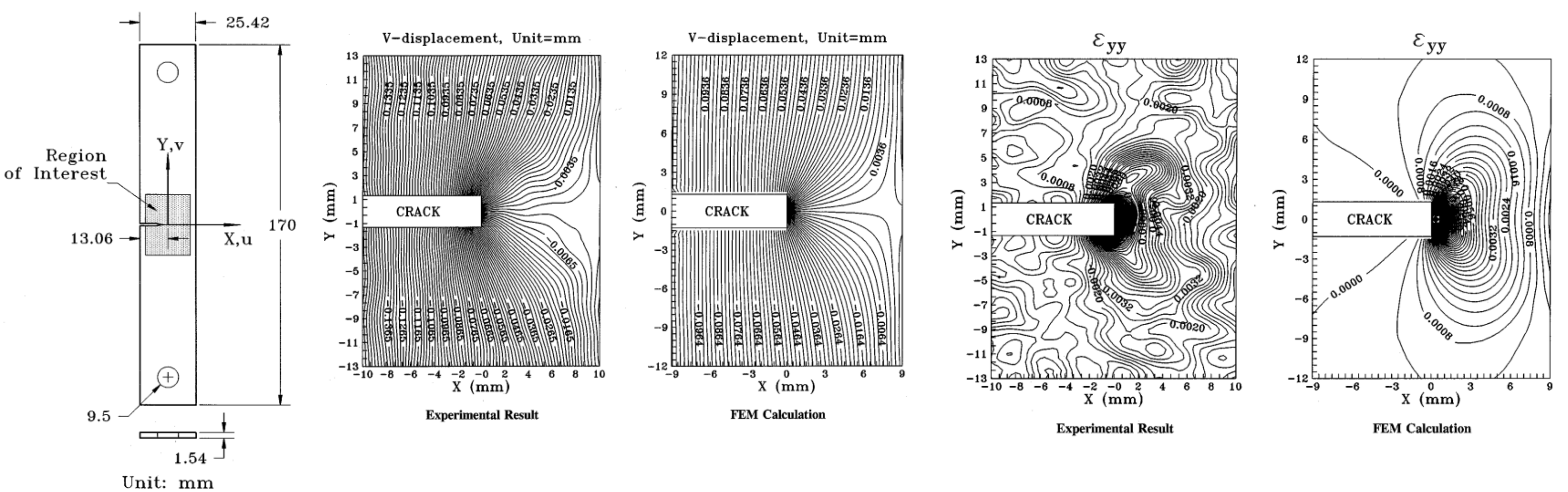

2D Image Correlation: Key Developments

- Ductile fracture at high mag.(1990-1994)

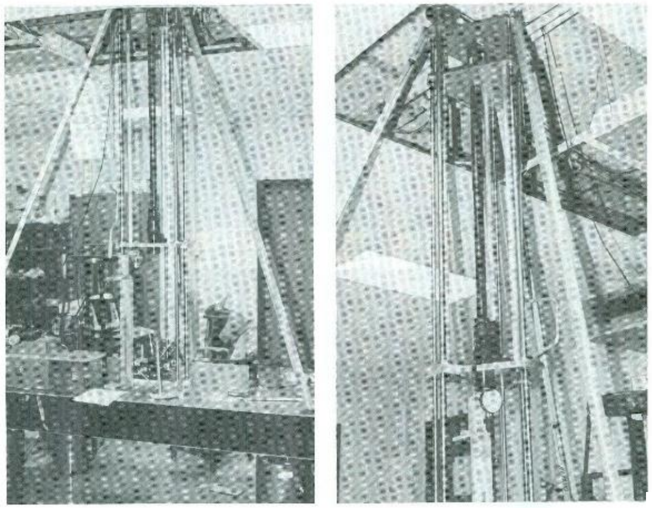

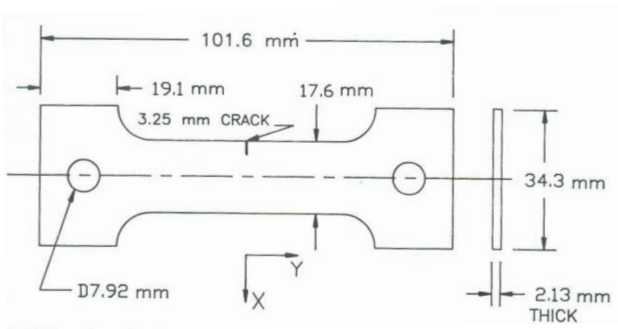

Δa = 0.00 mm

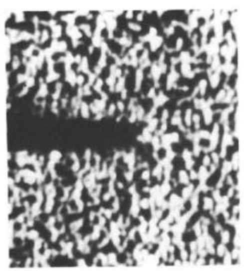

Δa = 0.00 mm

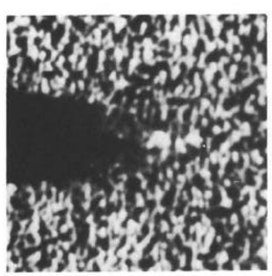

Δa = 0.67 mm

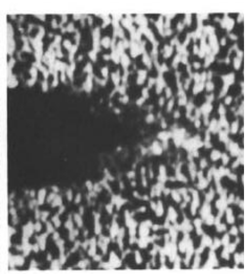

Δa = 0.82 mm

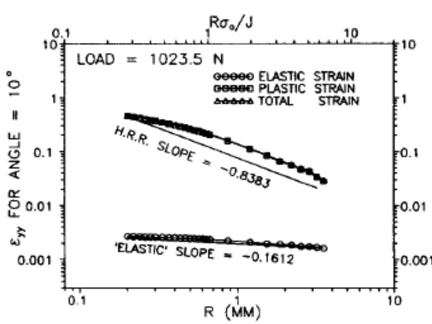

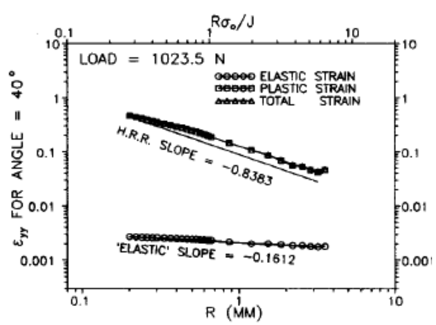

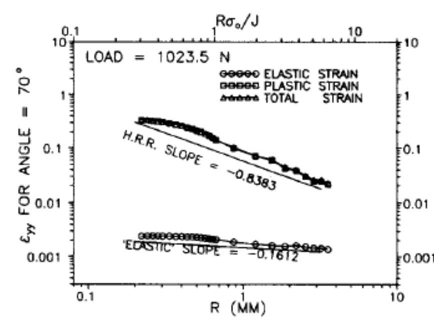

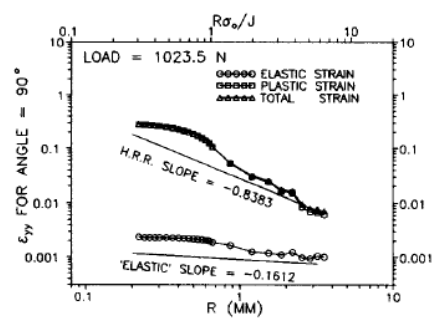

2D Image Correlation: Key Developments

University of South Carolina

- First two papers providing theoretical error predictions for 2D DIC
- INTERPOLATION INDUCED BIAS (1998-2000)

THEORY (cubic polynomial) SIMULATIONS

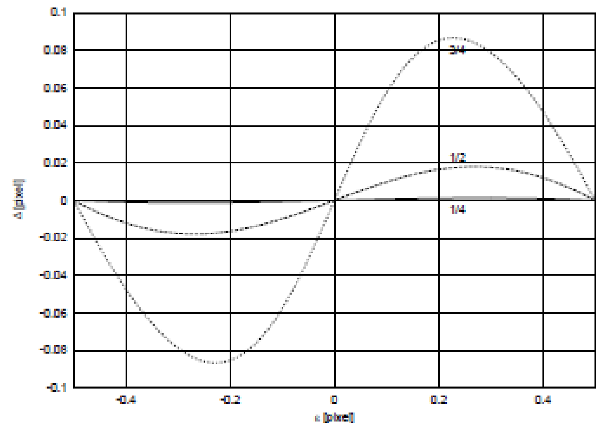

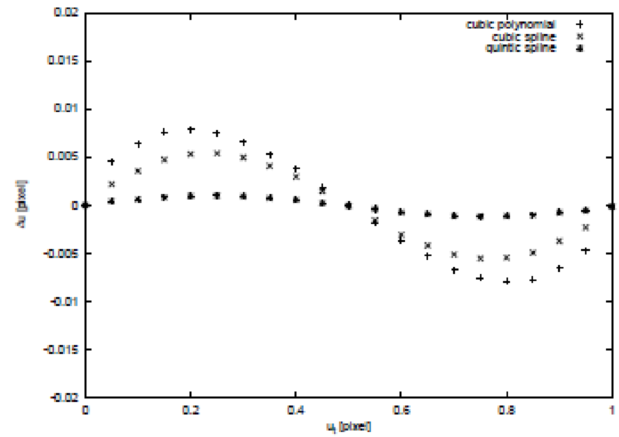

- VARIANCE AND NOISE-INDUCED BIAS (2005-2009)

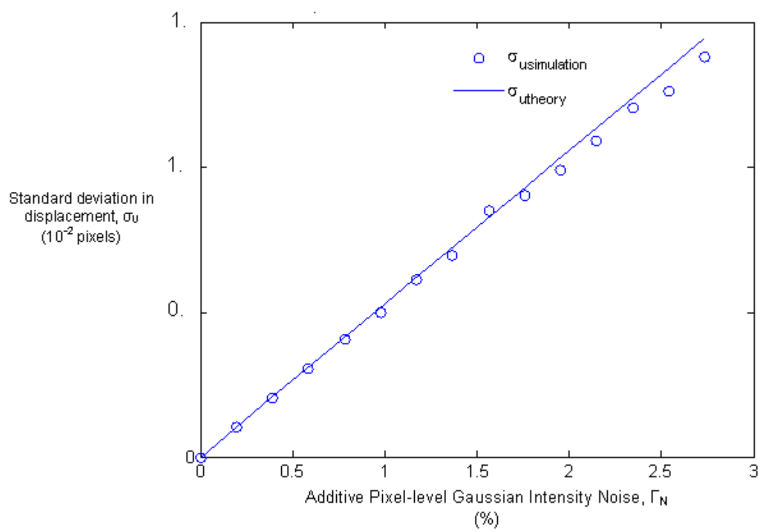

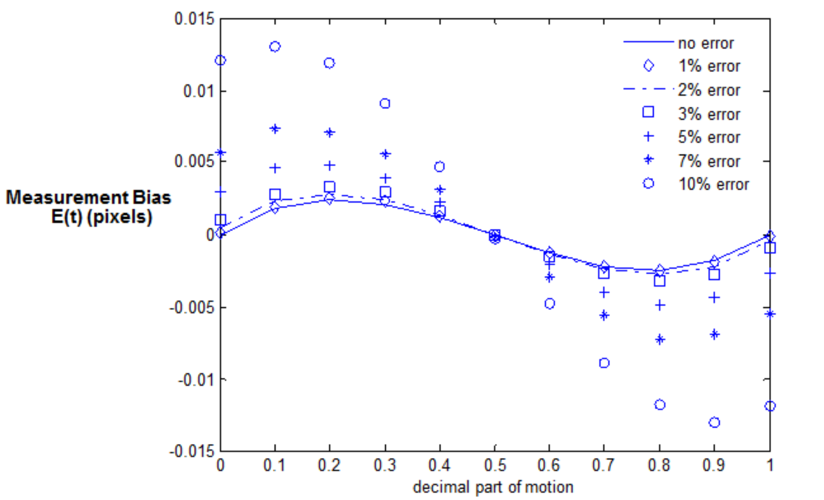

2D Image Correlation: Key Developments

- Simulation process for each sub-pixel translation.

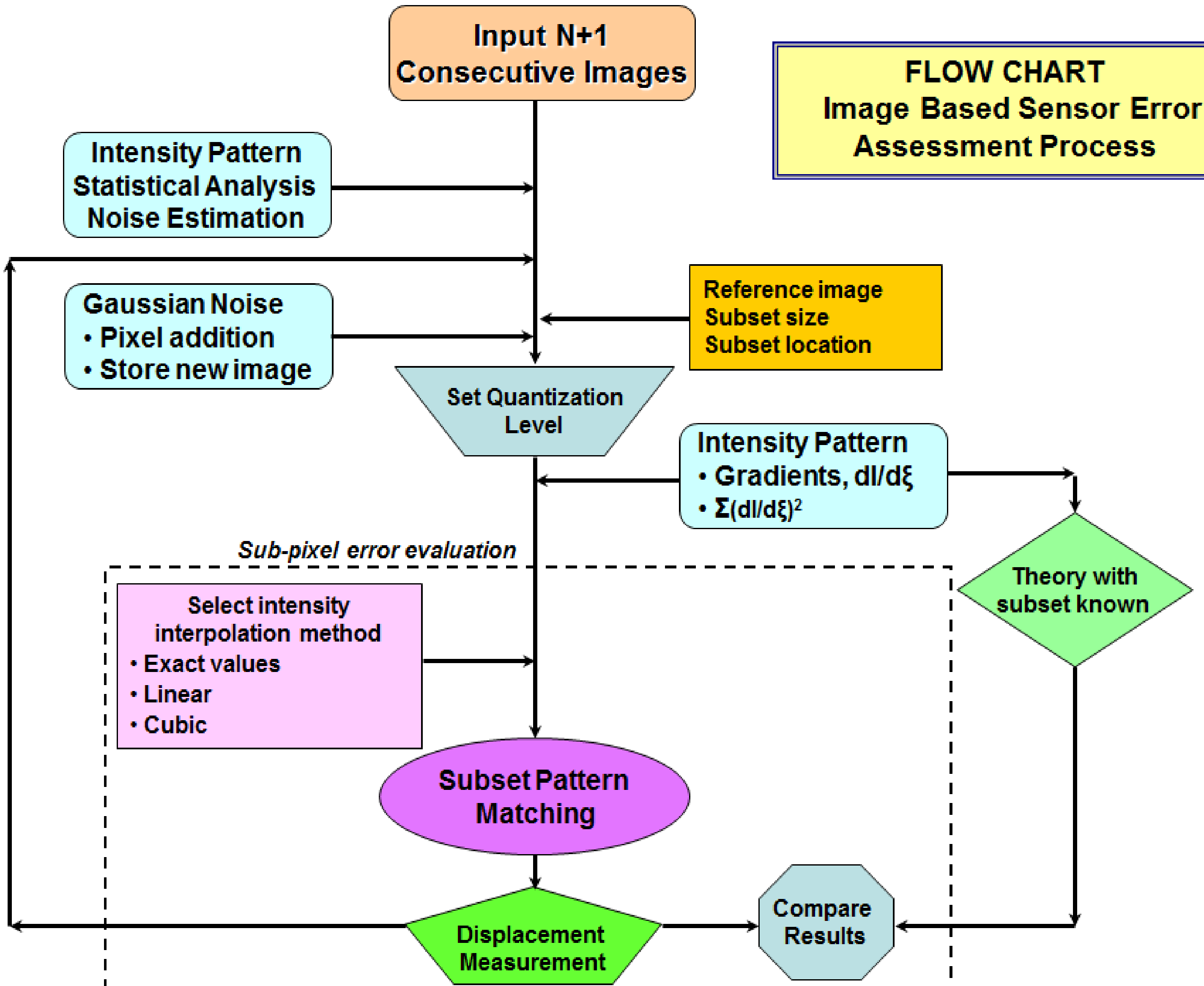

2D Image Correlation: Key Developments

- SEM DIC with distortion corrections (2003)

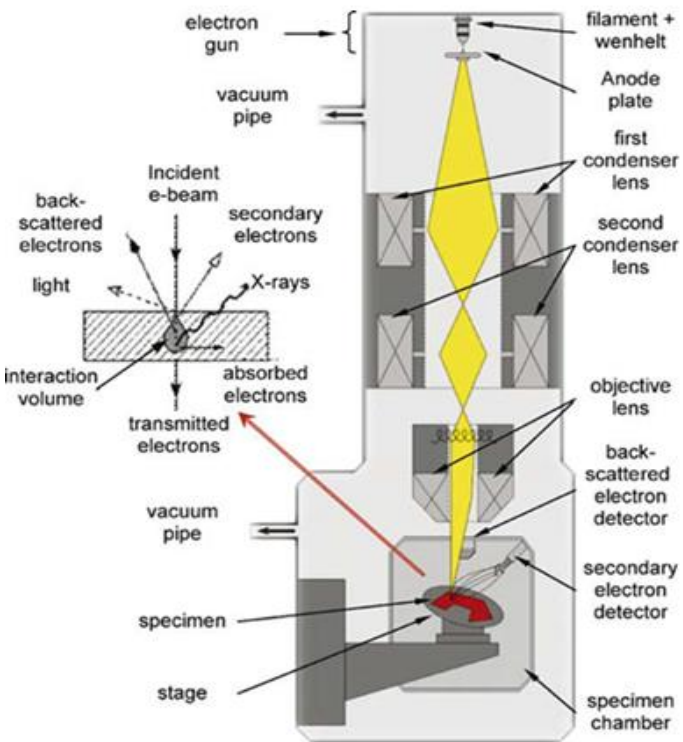

(1) Spatial distortion in an SEM which varies from experiment to experiment

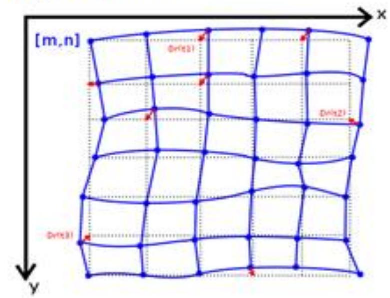

(2) Drift distortion which is non-linear and varies over time

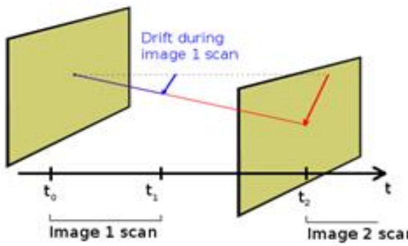

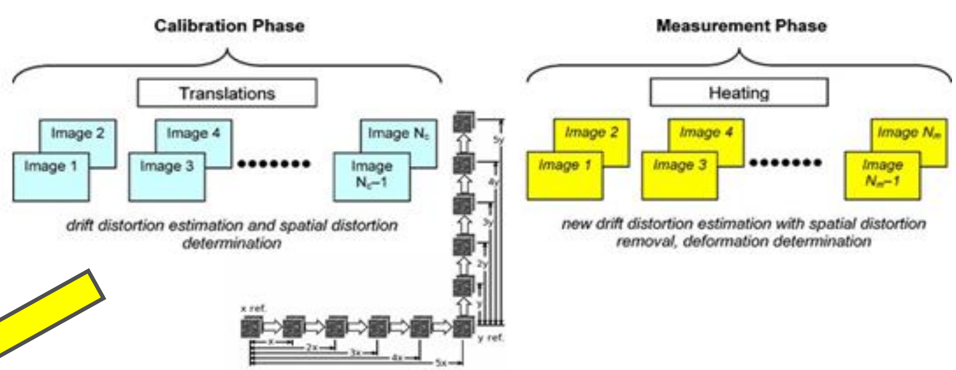

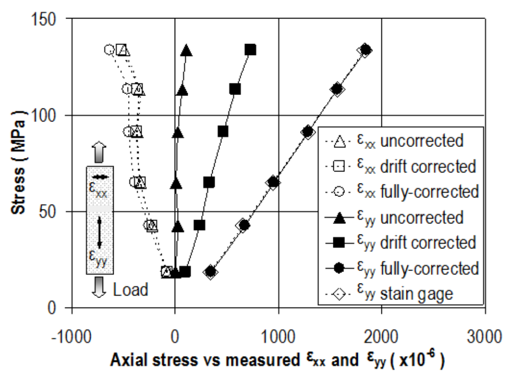

Fig. 9: Uniaxial stress versus axial strain and transverse strain for uncorrected, drift corrected and fully corrected image correlation data

3D Image Correlation: Basic Concepts

University of South Carolina

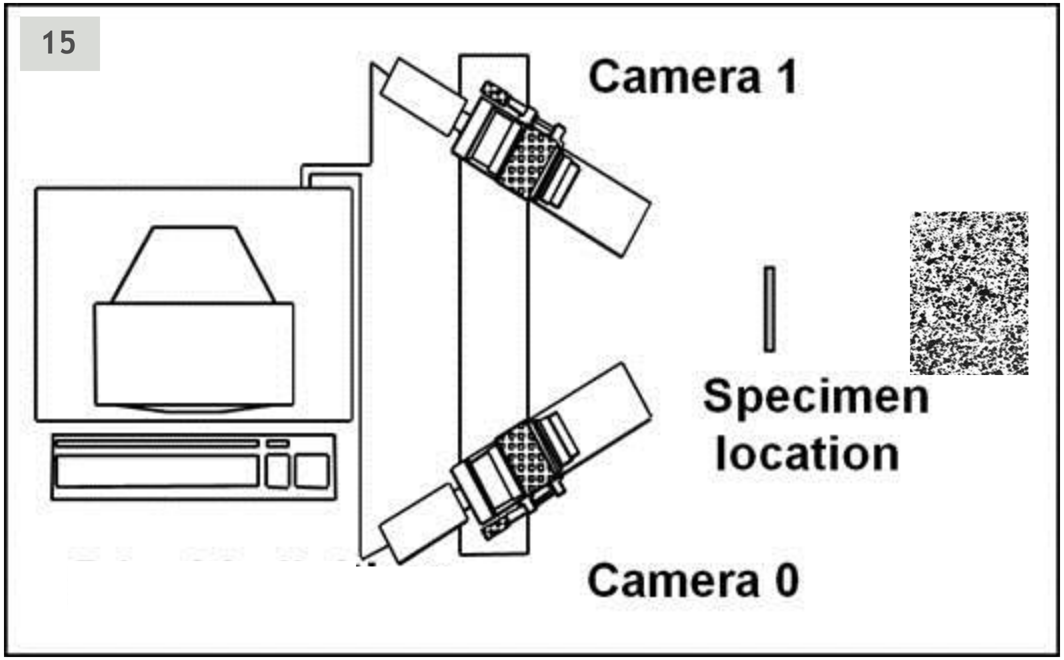

Two or more CCD cameras positioned to view same object area

- Specimen has a random pattern on its surface
- Uniform illumination is provided by white light sources
- General loading of specimen is allowed, while maintaining images of same object region in at least two cameras
- Images acquired simultaneously by all cameras

3D Image Correlation: Basic Concepts

University of South Carolina

General Remarks

- Full, three-dimensional displacement measurements obtained in laboratory and field conditions
- Calibration of camera system is required to convert image motions into accurate 3D measurements
  - Initial shape and 3D displacements are measured
- Data acquisition and data analysis procedures are well established
- Curved or planar objects from 0.50 mm to several meters in size
- Includes effect of perspective in image analysis
- High speed data analysis with data analyzed at > 3000 subset pairs per second
- Accuracy unaffected by large rotations or translations
  - Out-of-plane motion is measured, so does not affect accuracy of the in-plane measurements
- Accuracy of 3D displacement data is a function of camera system and camera noise level
  - Both variance and bias equations are available for estimating displacement errors
- Accuracy of 100 μs or smaller in strain on a point-to-point basis through differentiation of smoothed displacement data.

2D Image Correlation: Key Developments

University of South Carolina

- Early 3D vision system and 3D-DIC (1990-1994)

TABLE 1—CALIBRATION POINT LOCATIONS IN REFERENCE COORDINATE SYSTEM AND IMAGE POINT LOCATIONS IN COMPUTER-IMAGE COORDINATE SYSTEM COR ρ = 20 DEG

	Calibration Points			Image Points at Camera #1		Image Points at Camera #2	
	X	*Y*	*Z*	*H*	*V*	*H*	*V*
Point No.	(mm)	(mm)	(mm)	(pixel)	(pixel)	(pixel)	(pixel)
1	0.000	0.000	0.000	267.00	240.00	290.73	262.95
2	3.000	0.000	0.000	281.30	239.93	276.68	262.80
3	-3.000	0.000	0.000	252.96	240.15	304.56	262.89
4	-3.000	5.000	4.000	318.53	173.00	370.09	196.09
5	0.000	5.000	4.000	333.14	172.18	356.79	195.24
6	3.000	5.000	-4.000	348.03	308.57	342.93	331.02
7	-3.000	5.000	-4.000	318.39	307.80	369.80	330.13
8	-3.000	-5.000	-4.000	186.37	308.26	239.65	329.15
9	0.000	-5.000	-4.000	200.00	308.71	225.22	329.59
10	3.000	-5.000	-4.000	213.98	309.00	210.76	330.05
11	3.000	-5.000	4.000	214.00	170.39	211.01	195.01
12	0.000	-5.000	4.000	200.12	171.22	225.80	195.79
13	-3.000	-5.000	4.000	186.55	172.07	240.04	196.42
14	-3.000	-10.000	8.000	119.12	102.72	176.13	130.69
15	0.000	-10.000	8.000	132.28	101.30	161.25	129.32
16	3.000	-10.000	8.000	145.70	99.97	146.13	128.01
17	3.000	10.000	8.000	414.47	103.36	410.94	125.51
18	0.000	10.000	8.000	398.99	104.94	423.94	126.90
19	-3.000	10.000	8.000	383.76	106.24	436.79	128.09
20	-3.000	10.000	-8.000	383.49	375.00	436.34	398.63
21	0.000	10.000	-8.000	398.86	376.01	423.41	399.82
22	3.000	10.000	-8.000	414.25	377.04	410.21	400.99
23	3.000	-10.000	-8.000	145.35	379.50	145.06	397.24
24	0.000	-10.000	-8.000	132.00	378.44	160.25	396.12
25	-3.000	-10.000	-8.000	118.83	377.37	175.13	395.00

Note: The accuracy of calibration points is 0.001 mm; The accuracy of image points is 0.05 pixels

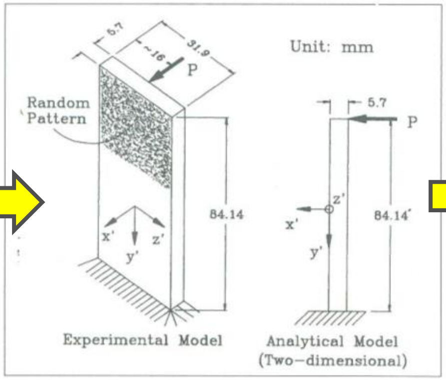

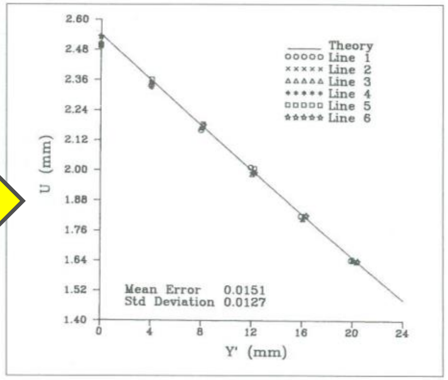

- Improving 3D-DIC systems for field studies. Aero-structures (1996-2003)

Local system

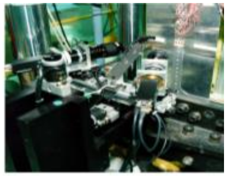

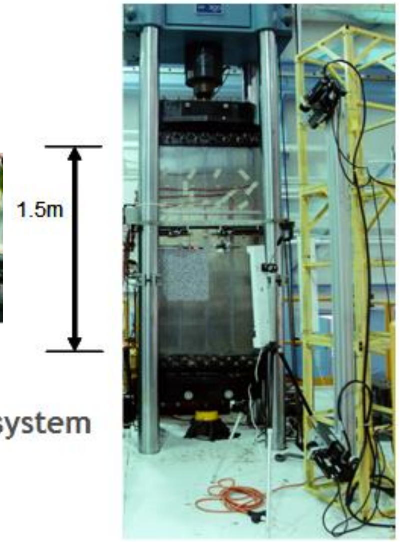

Global system

Experiments

Accuracy Estimate
- ±100 μm in-plane
- ±50 μm out of plane

Theory

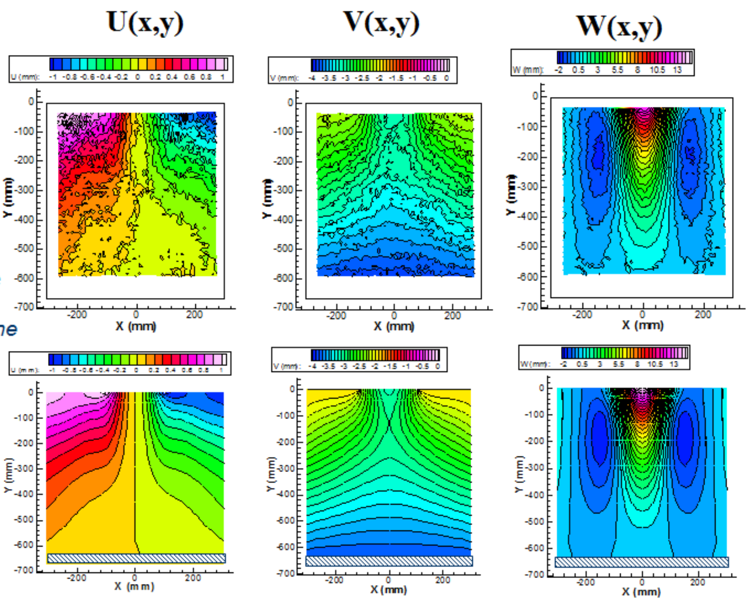

2D Image Correlation: Key Developments

- Error Propagation in 3D DIC (2006-2010)

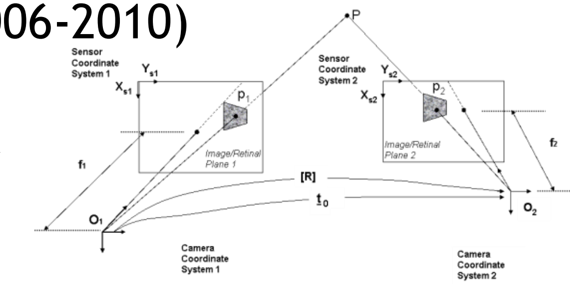

(x,y) = sensor position of a grid pt.

M_{ij} = matrix from sensor to 3D location

ξ = vector of 26 camera parameters used in M matrix

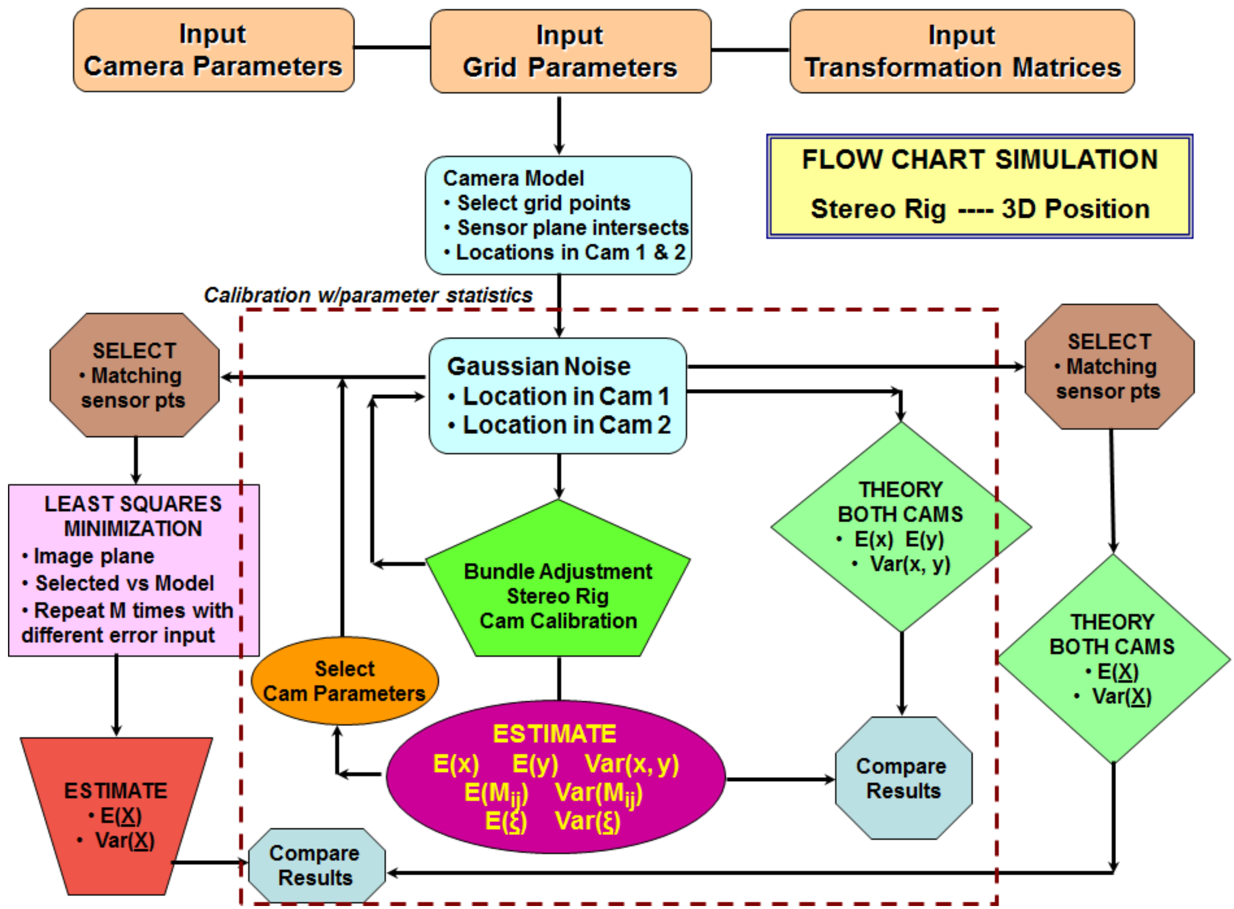

University of South Carolina

Volumetric DIC: Basic Concepts

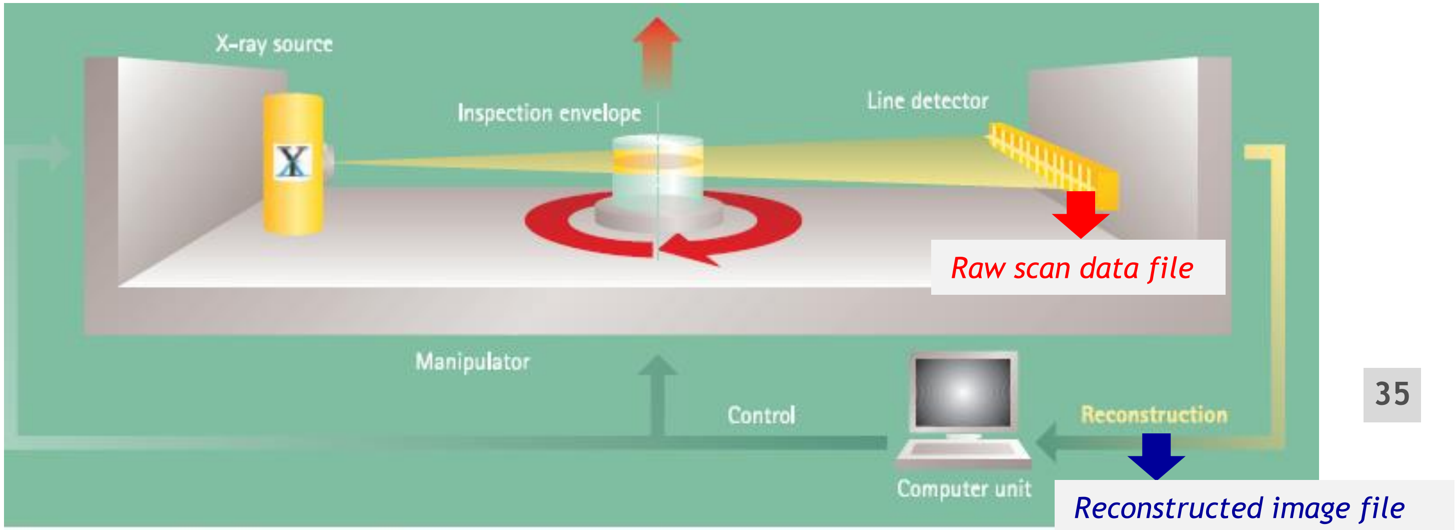

CT inspection using line detector

- System shown uses fan beam scanning approach
- Raw scan data file is digitally stored for each line and rotation angle
- Data is transferred to algorithms embedded in CT system and used to reconstruct images for each loading state
- Image data for each loading state used with optimization algorithms to determine internal deformations

Volumetric DIC: Basic Concepts

General Remarks

- Requires volumetric imaging system
- Pattern generally comes from natural internal sources, unless seeding of material is viable
  - When seeding material to improve pattern, may affect material response
- Image acquisition is slow, with lab CT images requiring up to several hours to complete high resolution scanning
- Noise levels are relatively high, with 3% noise or higher common in CT systems
- Data acquisition and image reconstruction procedures are well established, though prone to introduce artifacts
  - Image artifacts commonly seen in volumetric images can reduce accuracy of the matching process.
- Images can be obtained for small and large specimens
- Images are large, requiring efficient memory management and fast matching algorithms to reduce analysis time
- Accuracy nominally unaffected by large rotations or translations
  - Requires robust "initial guess" methods for estimating local motions
- Accuracy of +/-0.02 voxels in displacement on a point-to-point basis have been obtained in recent CT studies with high contrast patterns

2D Image Correlation: Key Developments

- First volumetric DIC Paper (BK Bay, 1999)

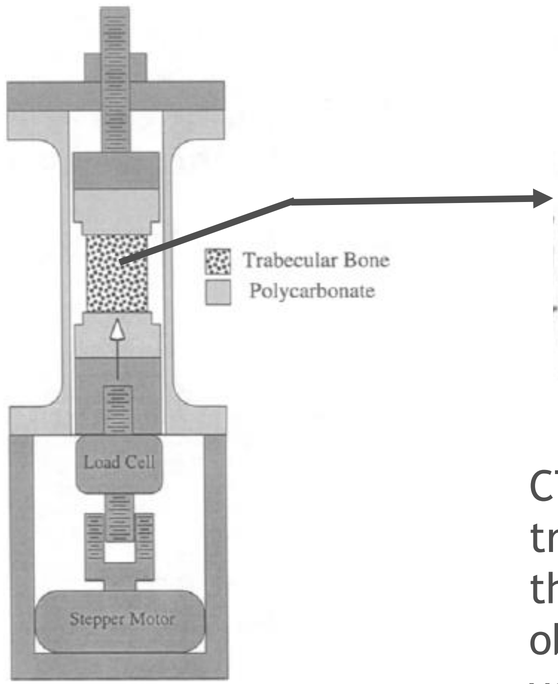

Fig. 1—The apparatus used for microCT scanning of trabecular bone samples under load

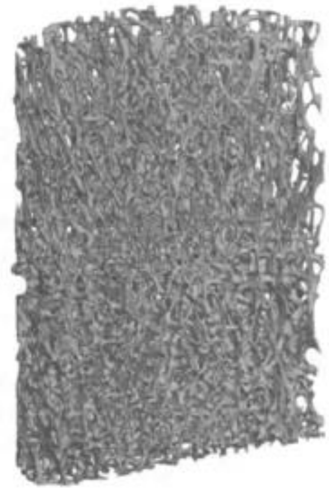

CT images of trabecular bone. Note the excellent contrast obtained throughout volume

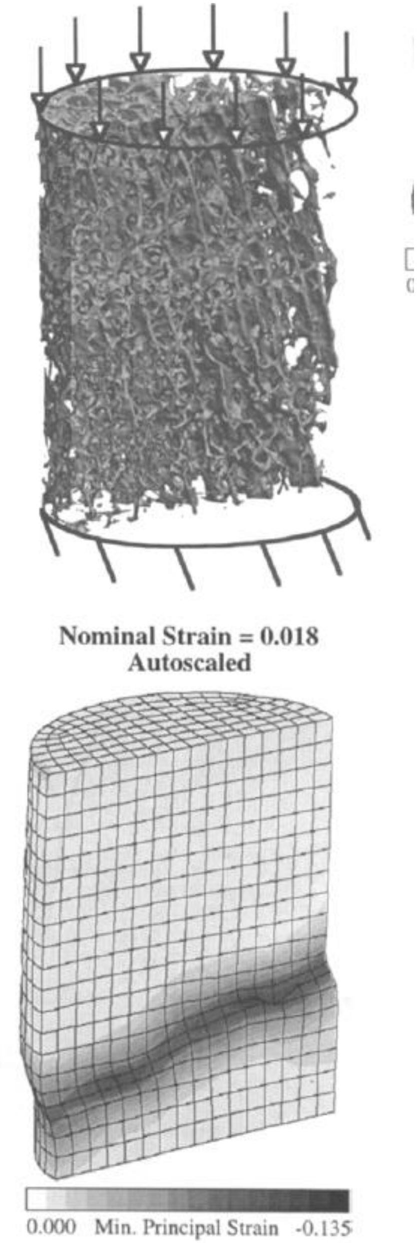

3D-DIC Applications

- Heterogeneous material
  - Woven glass-epoxy composite
  - Combined compression-bending loading
  - Large out-of-plane displacements
- Roofing Shingles
  - Background
  - Preliminary Experiments
  - Simulations

University of South Carolina

Woven Glass-Epoxy Composite

Material Specifics

- Thin sheet composite
- Glass-halogenated epoxy, NP-130
- Glass fibers approximately 7μm diameter
- Five-six layers of orthogonally woven composite in plain weave structure for 1m by 1.3m sheets
- Rectangular specimens removed with razor knife

NORPLEX MICARTA
High Performance Thermoset Composites

53

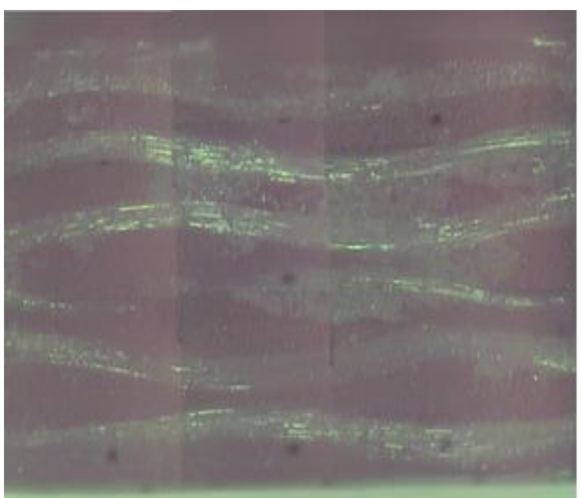

Edge View

Specimen geometry

- TH: 1mm
- W: 17mm
- L: 150mm.

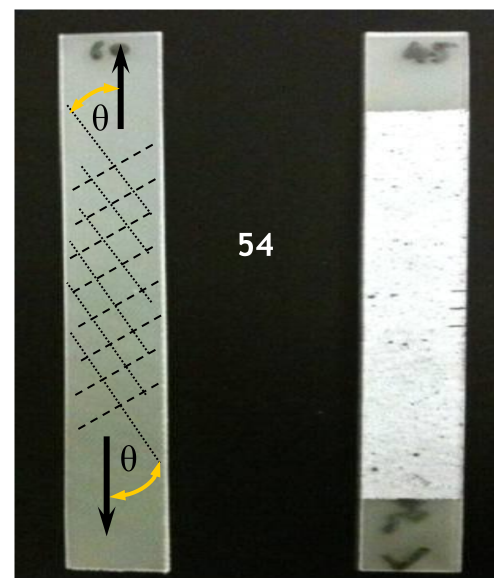

Woven Glass-Epoxy Composite

System Schematic

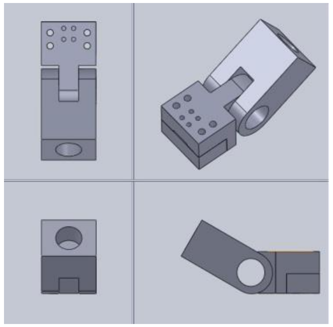

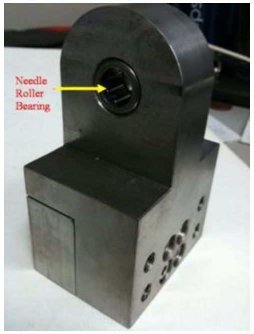

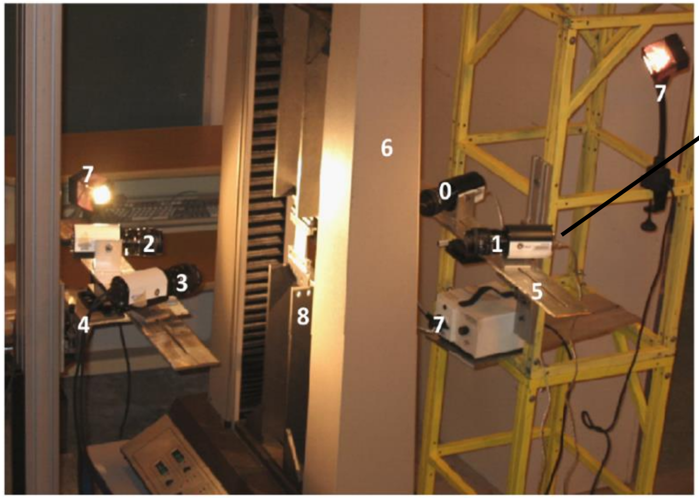

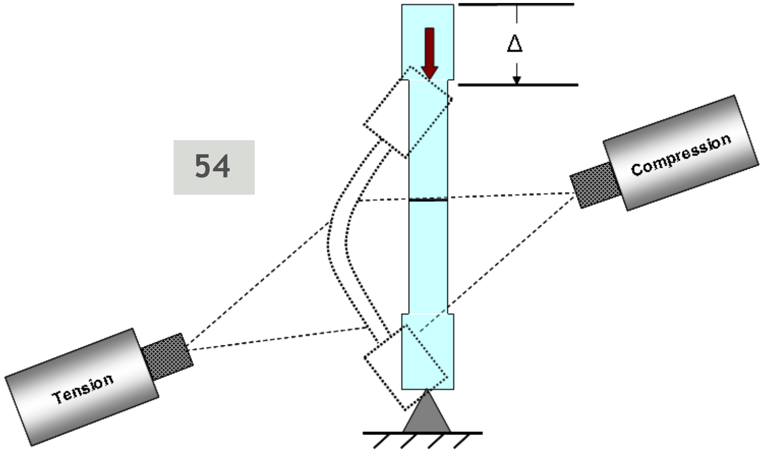

54

- Out-of-plane motions up to 40mm
- Compression side cameras
  - rotated counterclockwise by ≈20º
  - moved closer to specimen
  - specimen at front of focus volume
- Tensile side cameras
  - rotated clockwise by ≈20º
  - move away from specimen
  - specimen at back of focus volume

Woven Glass-Epoxy Composite

Axial strain on compression and tension surfaces during combined compression-bending loading for +/- 45º specimen.

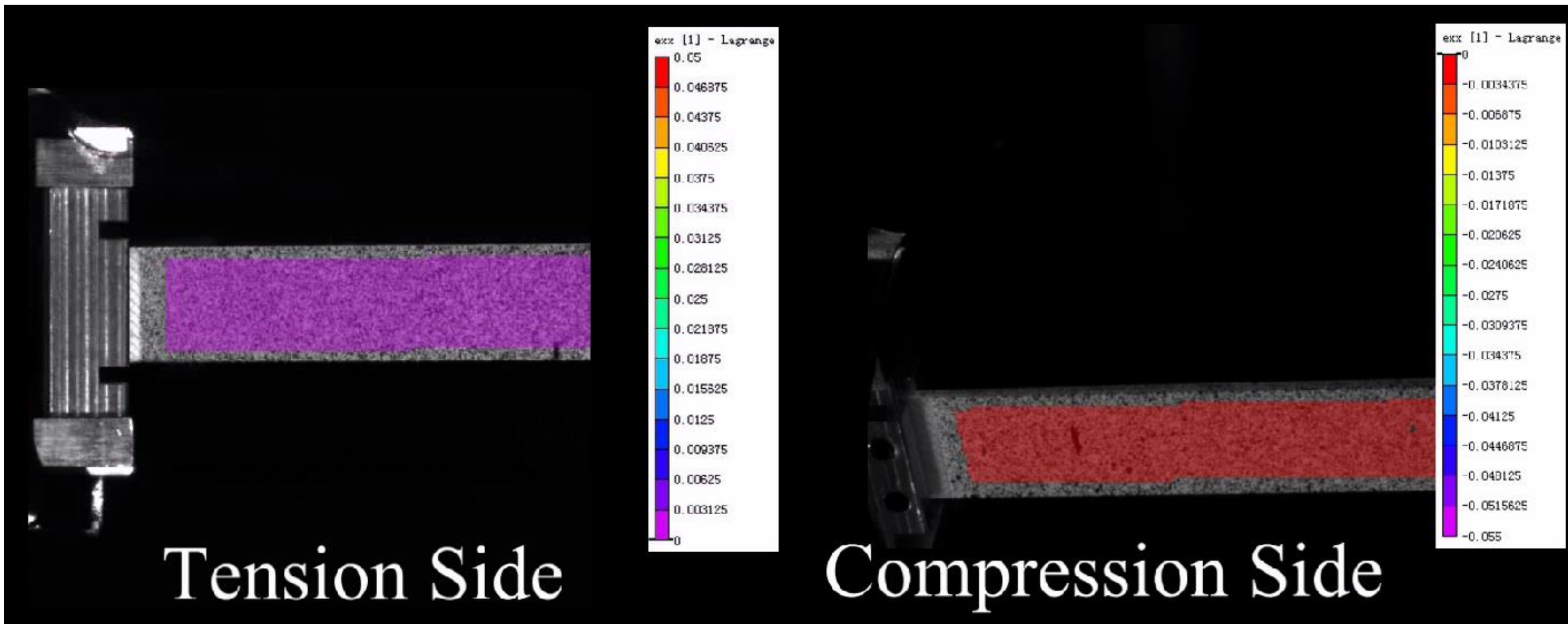

- Localized effects evident as w increases
- Critical regions have different spatial trends
    - Effect shown is muted for low fiber angles

Woven Glass-Epoxy Composite

Axial strain for Θ = 0^o and 20mm of axial displacement is in very good agreement with the large deformation results of the modified Drucker formulation on both surfaces.

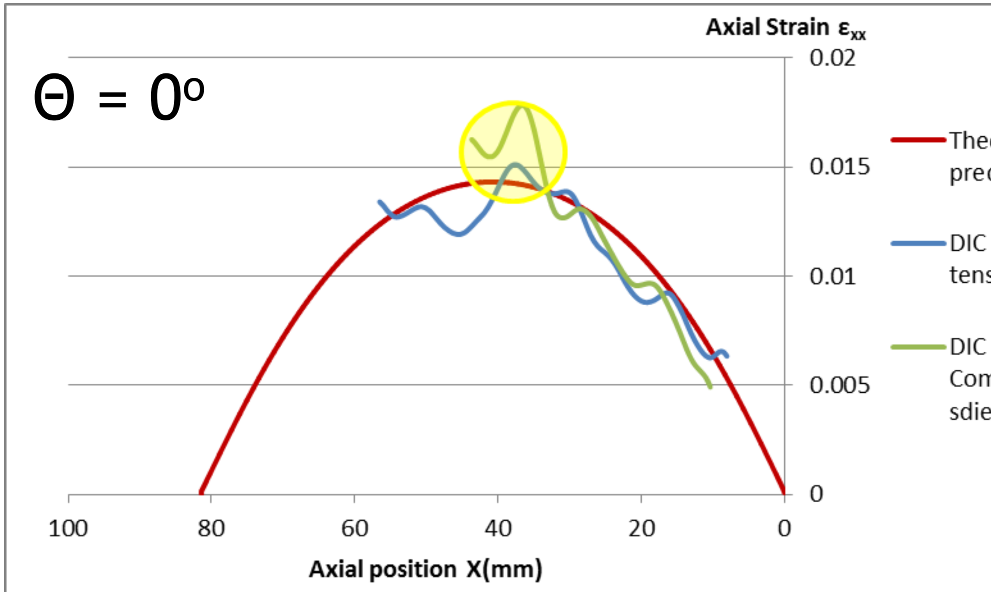

The elevated compressive strain in critical region appears to be due to localized damage, including fiber buckling and matrix failure.

University of South Carolina

Woven Glass-Epoxy Composite

University of South Carolina

Effective stress vs effective strain in critical region near mid-span of specimen

$$\tilde{\varepsilon}_\theta = \frac{\varepsilon_\theta}{h(\theta)} \quad , \qquad \tilde{\sigma}_\theta = \sigma_\theta h(\theta)$$

$$h(\theta) = \sqrt{\frac{3}{2}[\cos^4(\theta) + \frac{d_2}{d_1}\sin^4(\theta) + \frac{d_3}{d_1}\sin^2(\theta)\ \cos^2(\theta)]}$$

$$d_1 = \frac{1}{E_1},\ d_2 = \frac{1}{E_2}\quad d_3 = \frac{1}{G_{12}} - \frac{2\upsilon_{12}}{E_1}$$

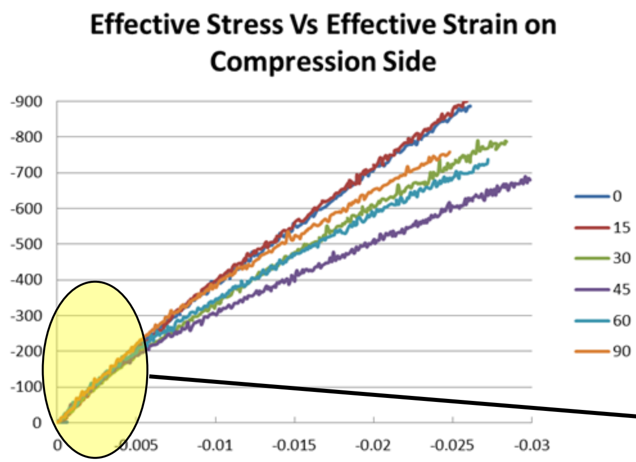

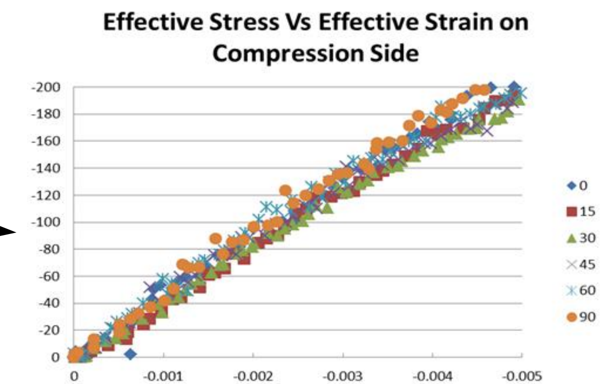

Figure 14

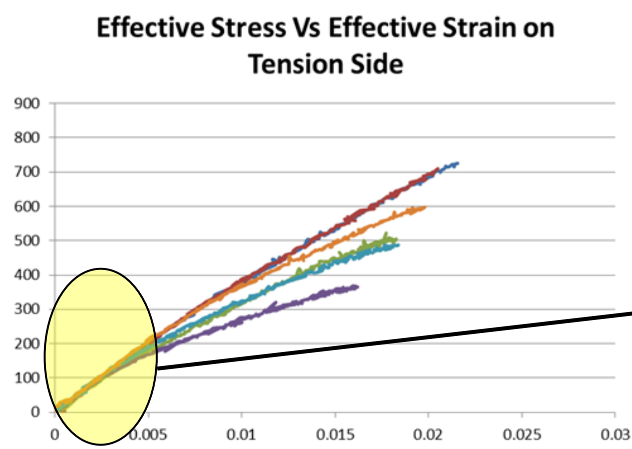

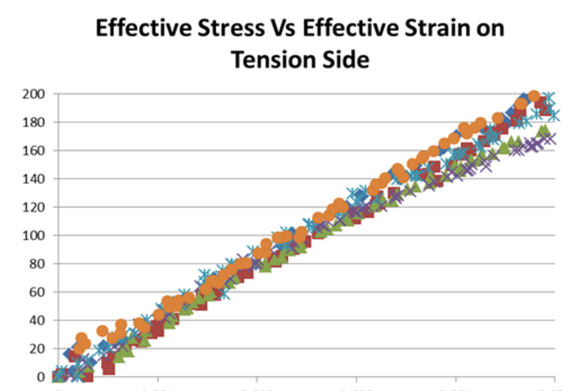

Woven Glass-Epoxy Composite

- **FE Simulations and Large Deformations**
  - Abaqus
  - Hashin damage model
  - 5 layers through total thickness-laminate construction modeled (not woven)
  - Alternating orthogonal fiber directions for layers (0-90-0-90-0) assumed
    - Layers modeled as individual orthotropic material (depending upon orientation of “fibers” relative to loading), with linear-elastic response and damage accumulation.
  - Hashin model parameters selected based on (a) literature data for glass-epoxy specimens of similar construction and (b) fitting of off-axis P-δ response of bending-compression spencimens.
    - Fibers are not modeled.

Woven Glass-Epoxy Composite

University of South Carolina

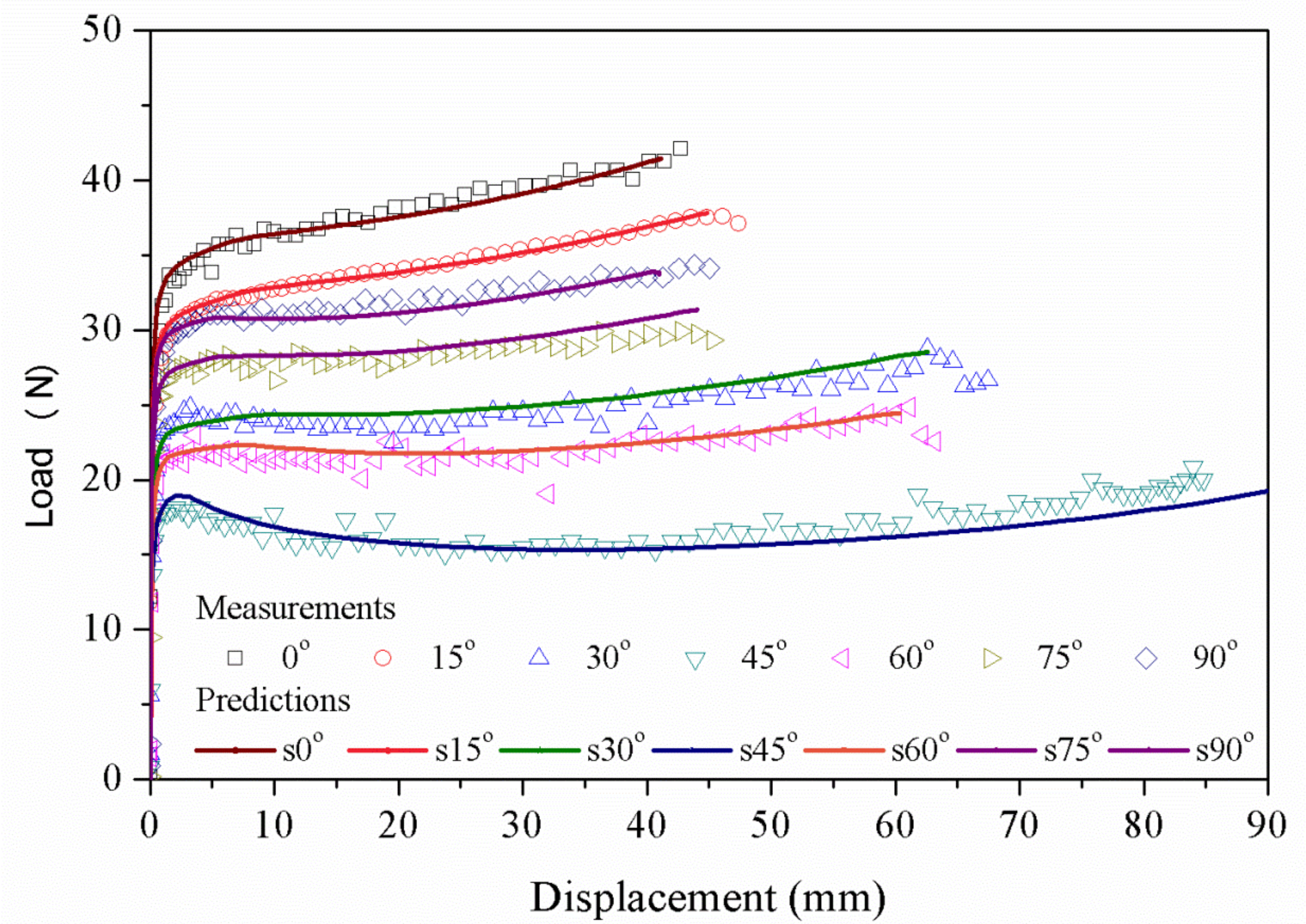

- Differences between 15 and 75; 30 and 60 apparently due to CT-observed difference in fiber number in 0 and 90 orientations

Coordinate System

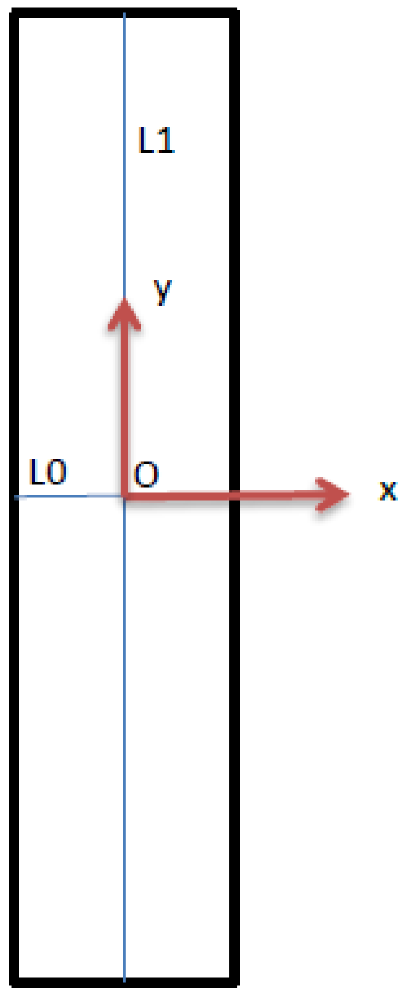

e_{xx} along L0

e_{yy} along L1

Front surface (compression side) of specimen

Woven Glass-Epoxy Composite

0°

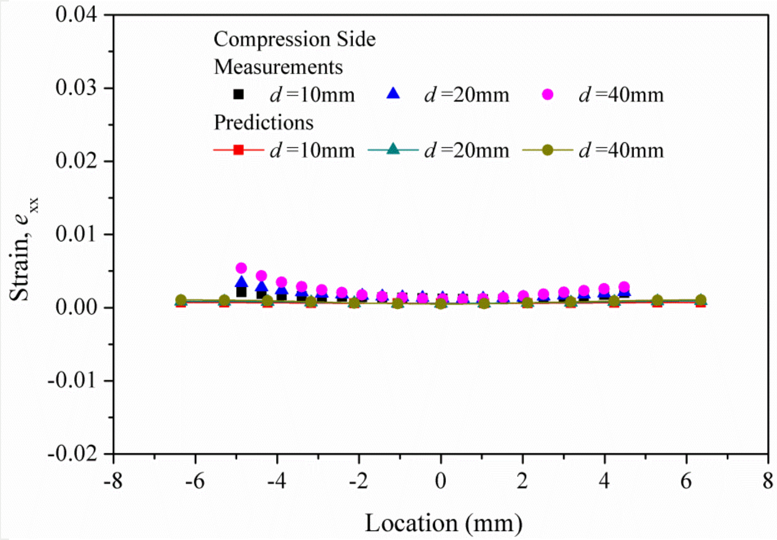

Compression side e_{xx}

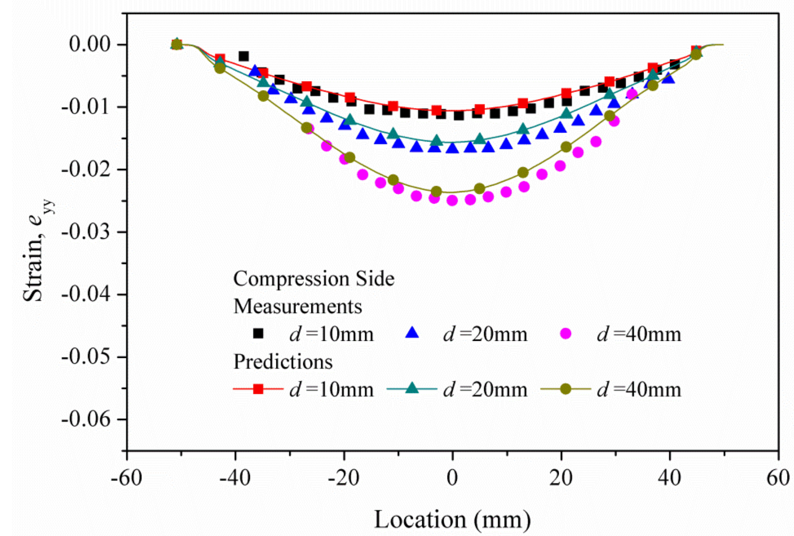

Compression side e_{yy}

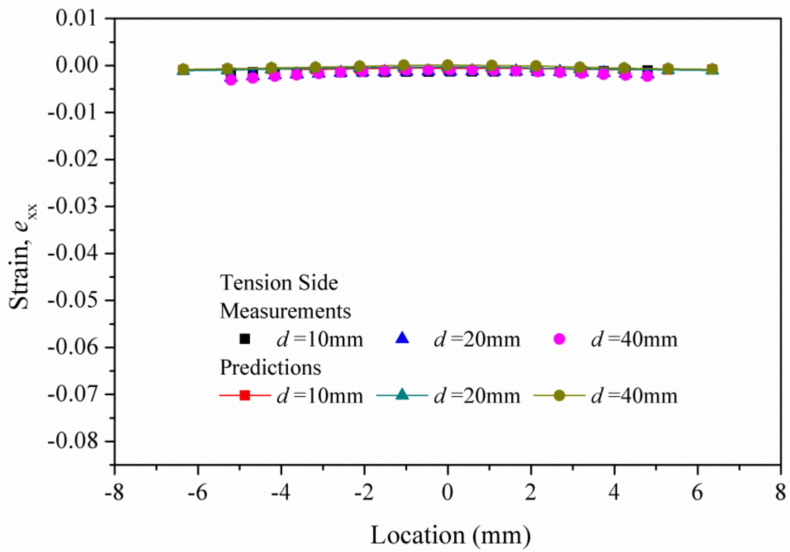

Tension side e_{xx}

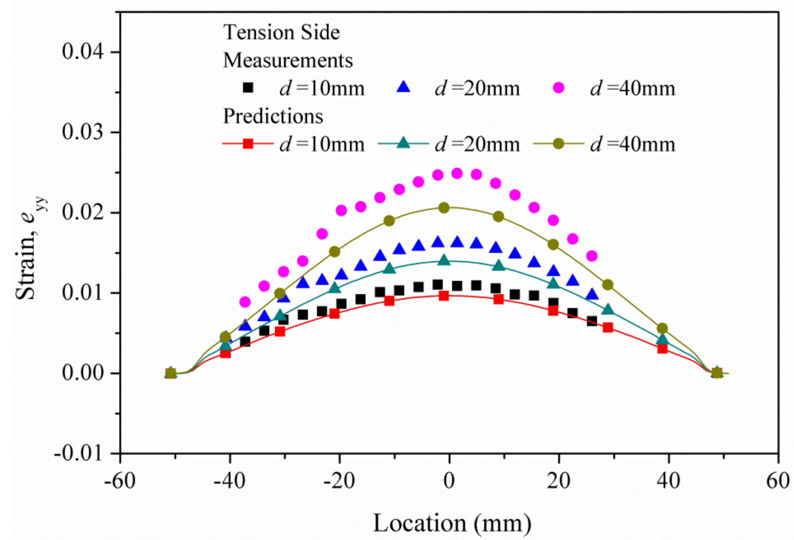

Tension side e_{yy}

Woven Glass-Epoxy Composite

University of South Carolina

60°

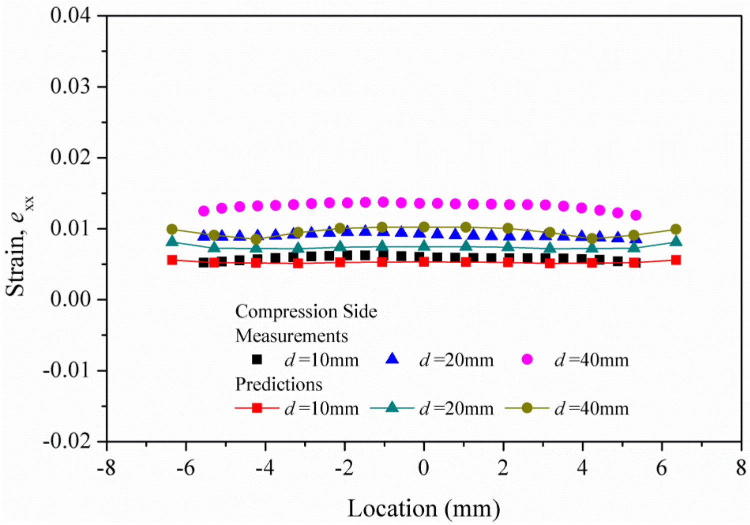

Compression side e_{xx}

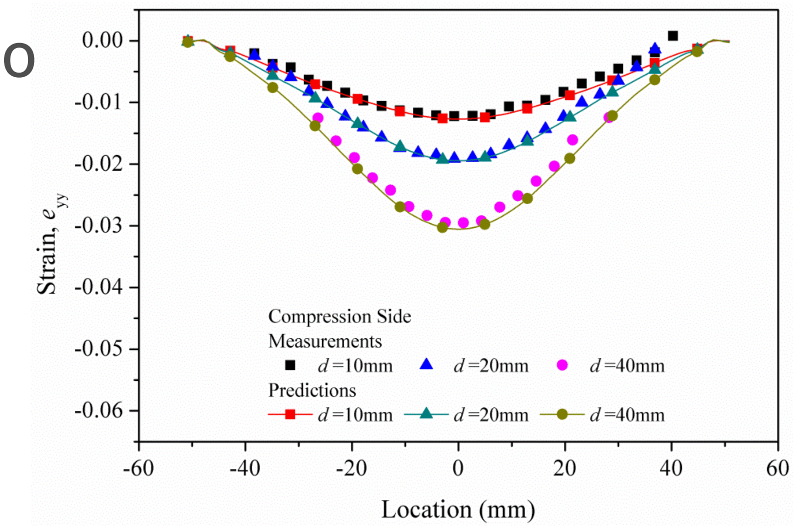

Compression side e_{yy}

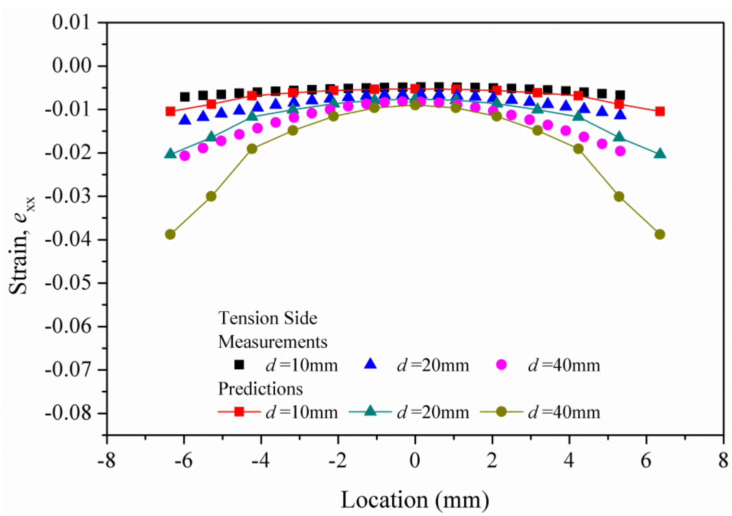

Tension side e_{xx}

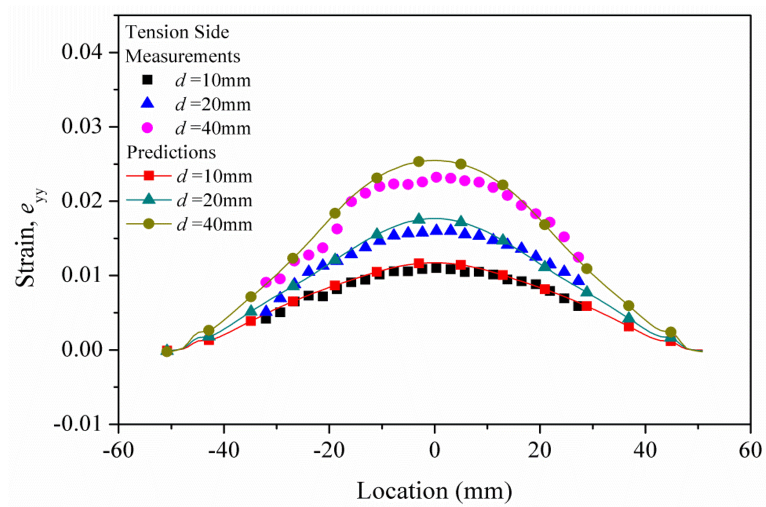

Tension side e_{yy}

Woven Glass-Epoxy Composite

60° at D = 40 mm, Tension side

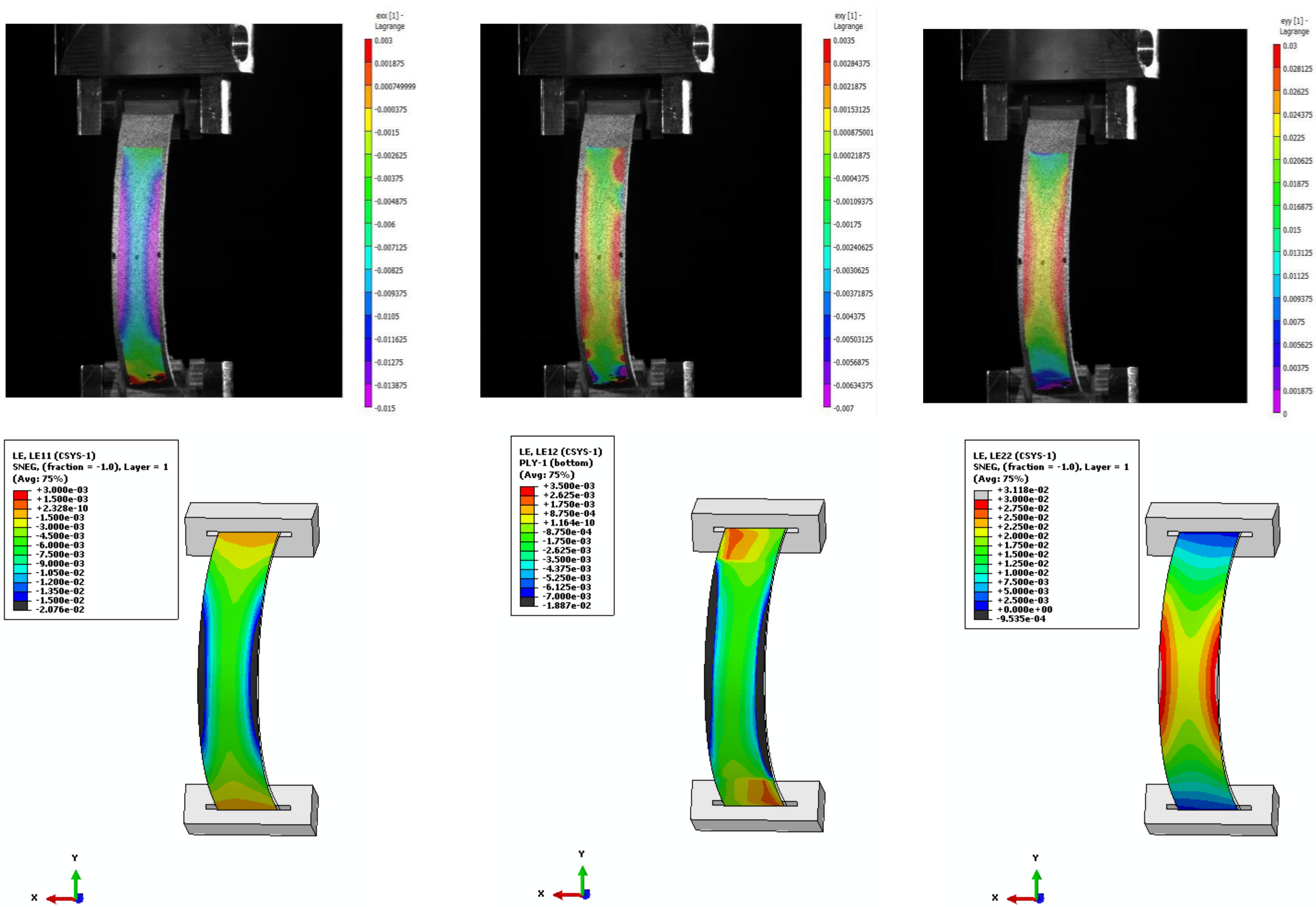

University of South Carolina

Woven Glass-Epoxy Composite

60º at D = 40 mm, Compression side

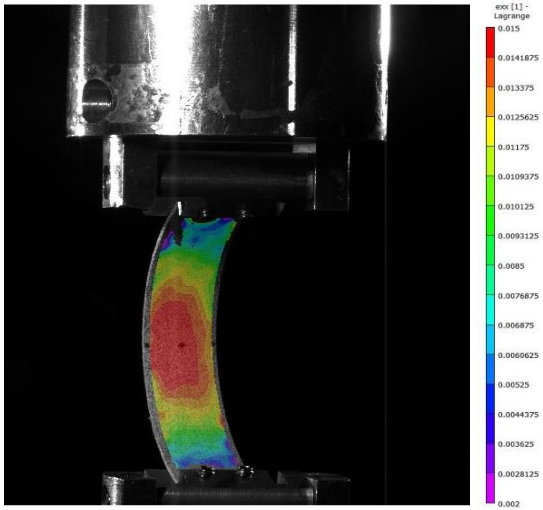

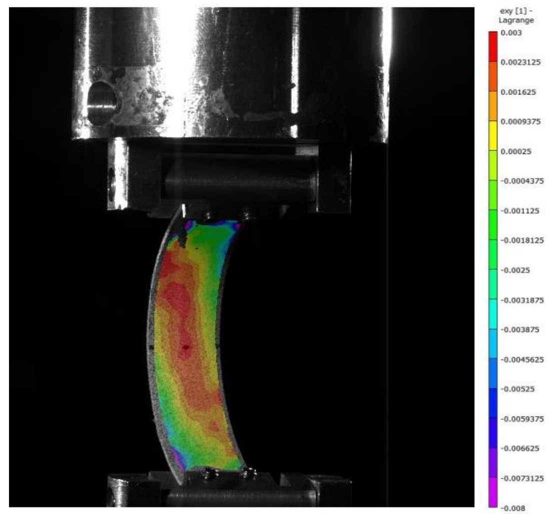

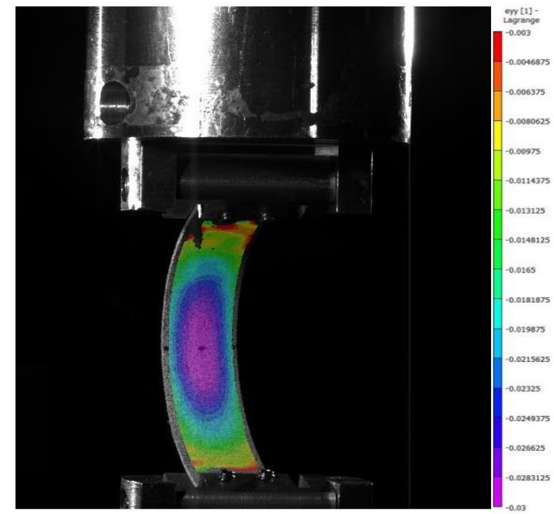

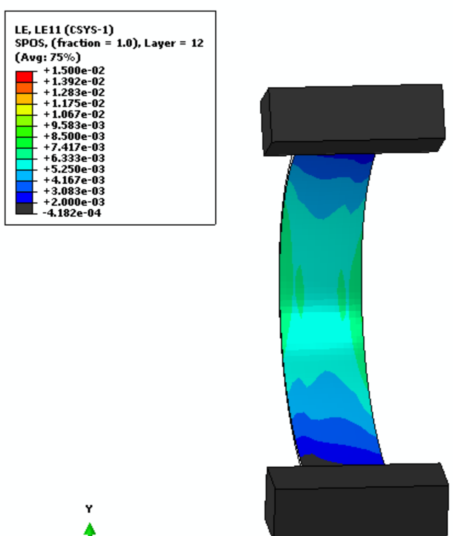

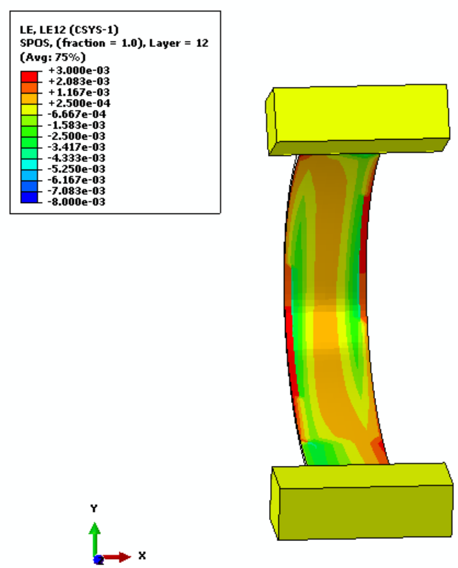

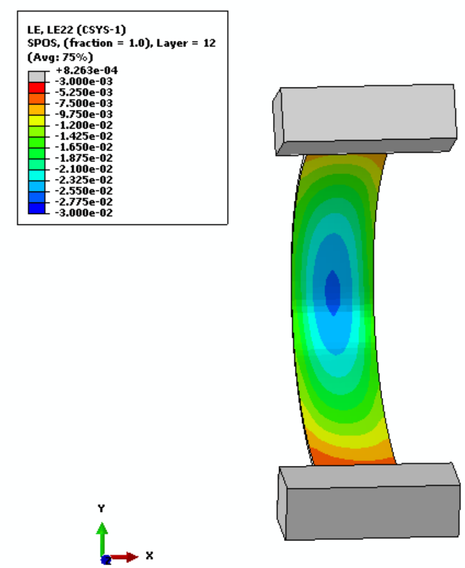

Applications

- Heterogeneous material
  - Woven glass-epoxy composite
  - Combined compression-bending loading
  - Large out-of-plane displacements
- Roofing Shingles
  - Background
  - Preliminary Experiments
  - Simulations

University of South Carolina

Roofing Shingles

- Roof asphalt shingles
  - The most common type of sloped-roof cover for residential construction in the US
  - Shingles consist of:
    Two layers of asphalt, fiberglass mat and granules
  - Sealing strip (introduced in the 1950s):
    - ✓ Minimizes the water penetration
    - ✓ Resists against wind-induced uplift

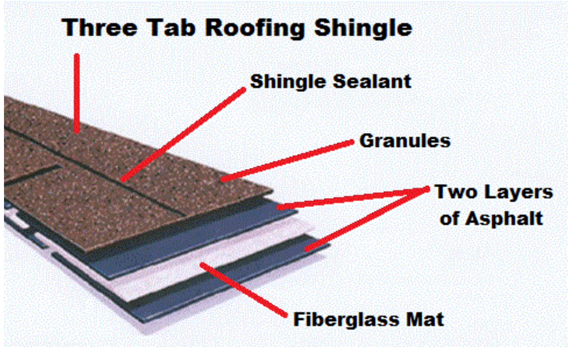

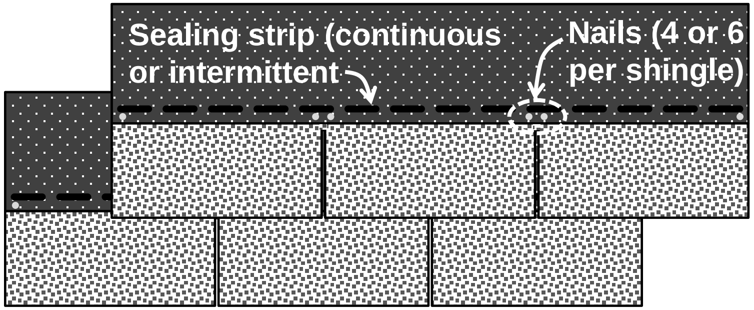

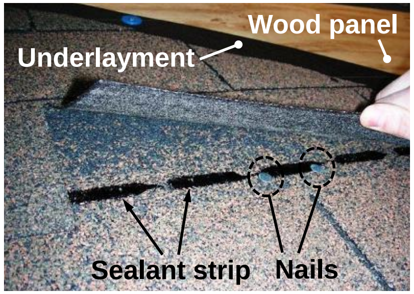

Roofing Shingles

Experimental Program

- 3D-DIC setup and wind load

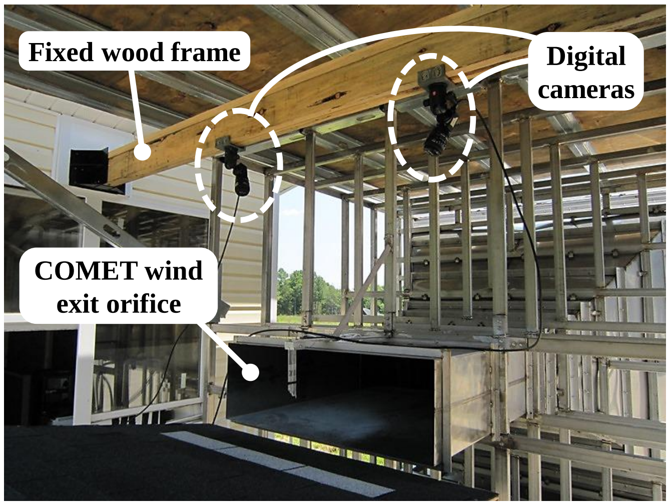

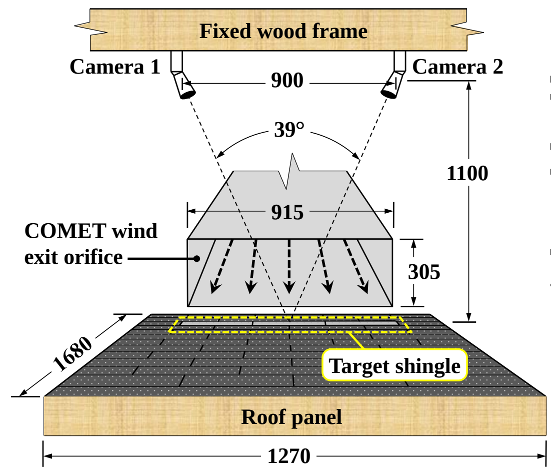

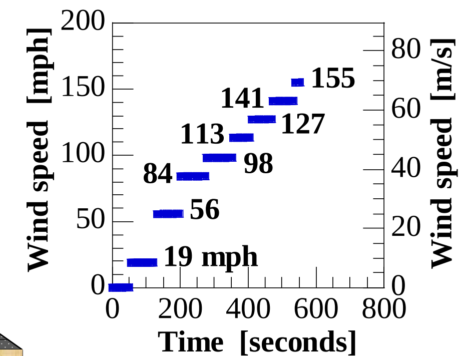

- Cannot paint surface due to stiffening effect on soft shingle material
- Cameras: Two 5 MP (Point Grey Grasshopper GRAS-50S5M-C)
- Lenses: 28-mm lenses (AF Nikkor 28 mm f/2.8D)
- Cameras were mounted on a fixed wood frame to minimize wind-induced vibrations
- Roof cover was built to minimize changes in ambient light
- 5 Hz frequency was used to acquire and store thousands of images

Roofing Shingles

- 340kmph wind. Time sped up by 10X.
- Audio turned off due to high dB noise.

University of South Carolina

Roofing Shingles

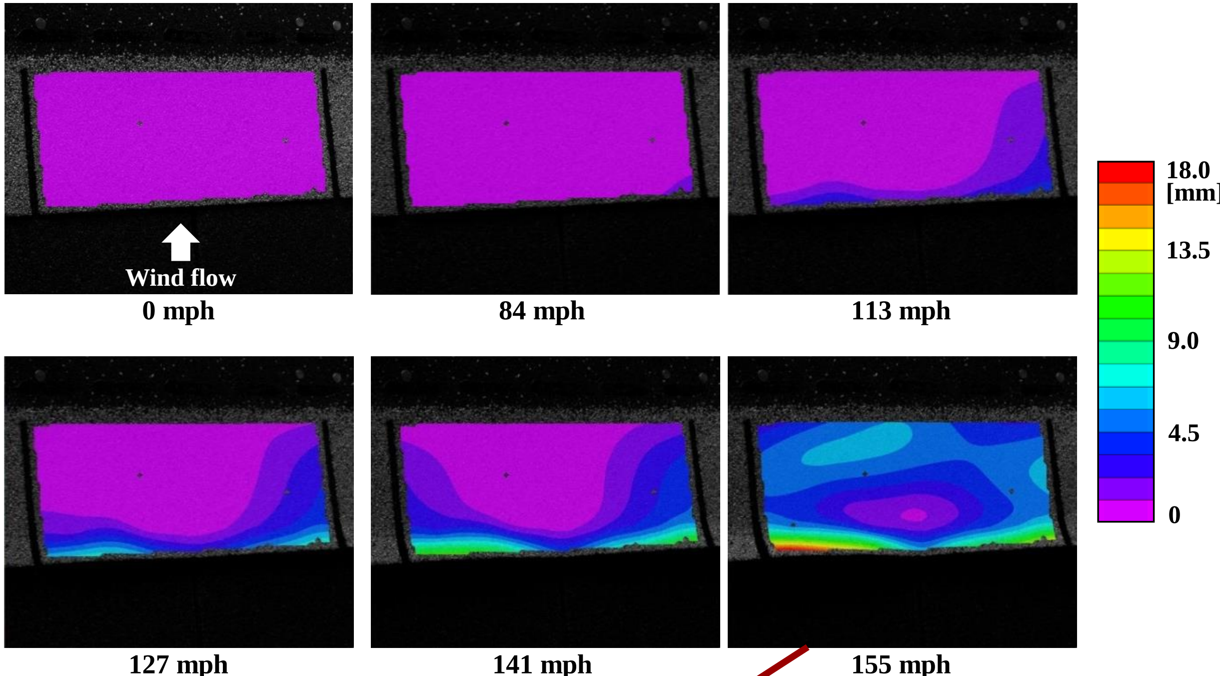

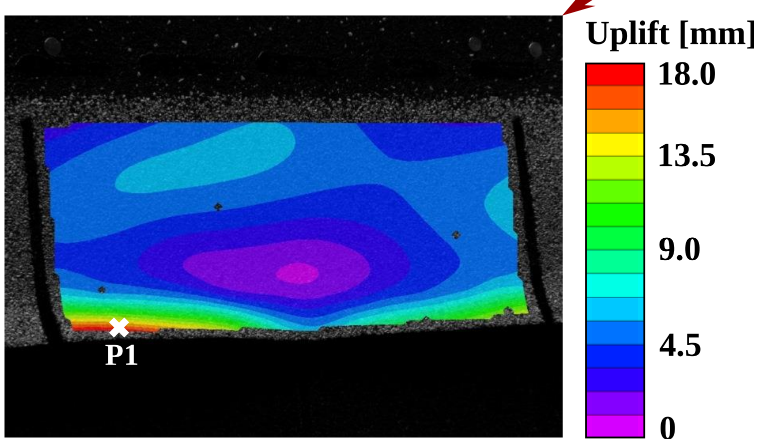

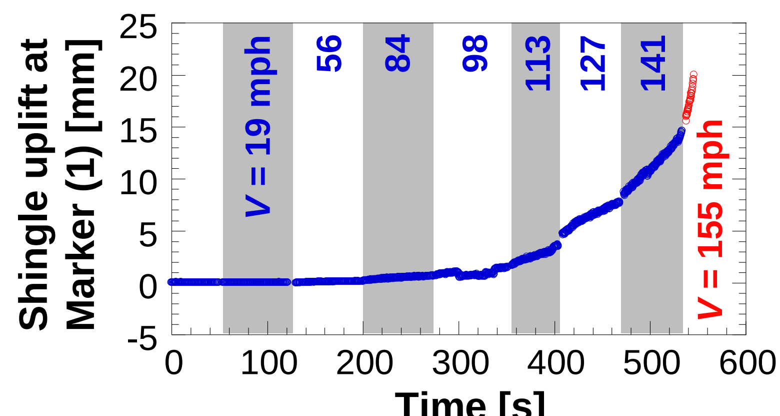

Roofing Shingles

University of South Carolina

Simulation of Shingle Response and Sealant Separation

- Beam on elastic foundation (BOEF) model is employed with finite sealant
  - "Foundation" represents effect of sealant material
  - Assume elastic response throughout deformation process. Beam and sealant lengths and properties obtained experimentally from commercially available shingle samples.
  - Uplift pressure p_1 measured independently for winds up to 200km/hr
  - Energy release rate at each edge of sealant strip is $\frac{1}{2} S v_2^2$
  - Drag force, P, not included in these results
  - Solution requires determination of 12 parameters

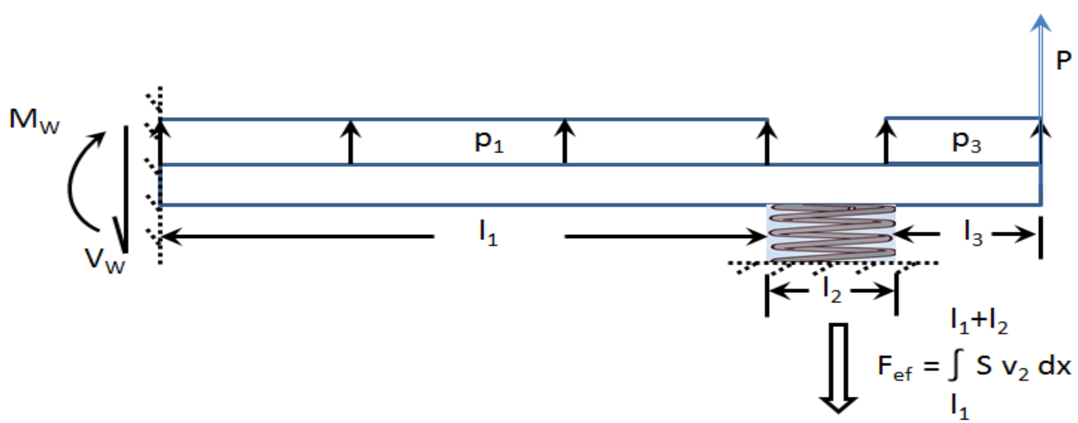

Roofing Shingles

University of South Carolina

Preliminary Experiments

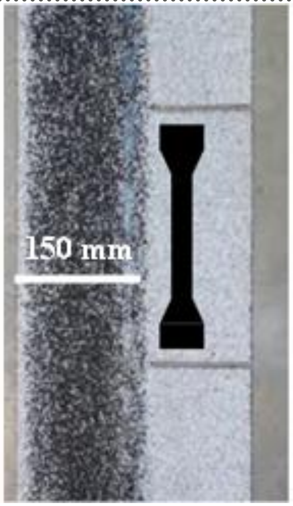

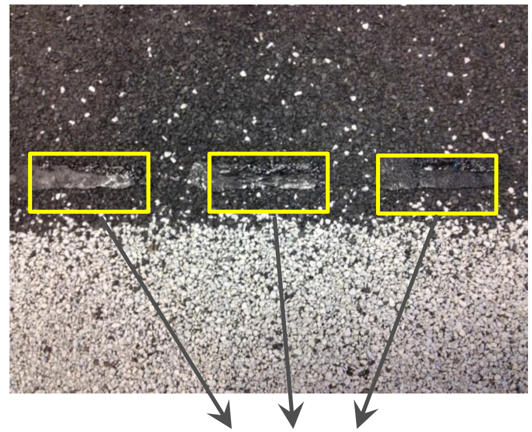

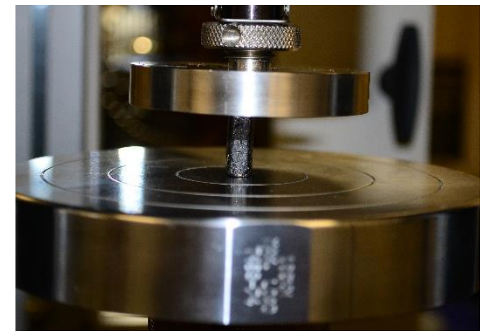

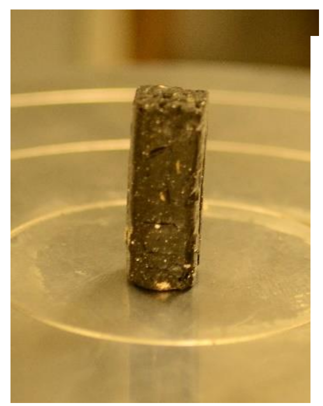

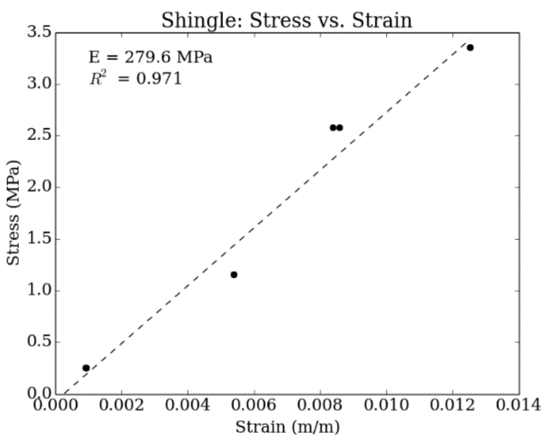

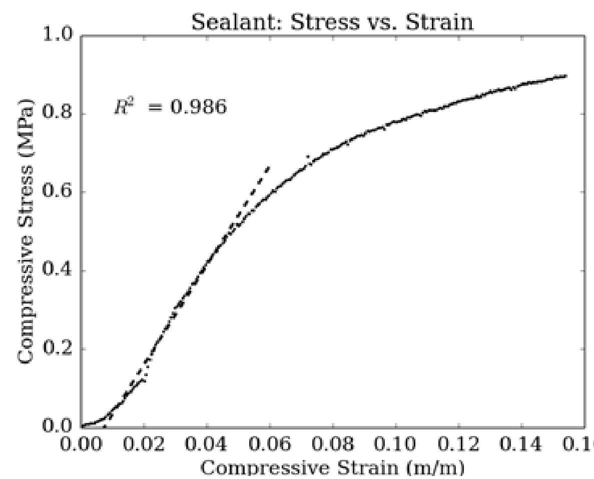

Compressive axial stress vs. axial strain measurements for sealant specimen at 23°C.

Shingle length, $0 \leq l_1 \leq 0.1204$ m
Sealant length, $l_2 = 0.0127$ m
Overhang length, $l_3 = 0.0254$ m
Sealant thickness: t = 2.8 mm
BOEF Sealant Parameter: S = 4.53Gpa m^{-1}

Roofing Shingles

Simulation Results-Energy Release Rate

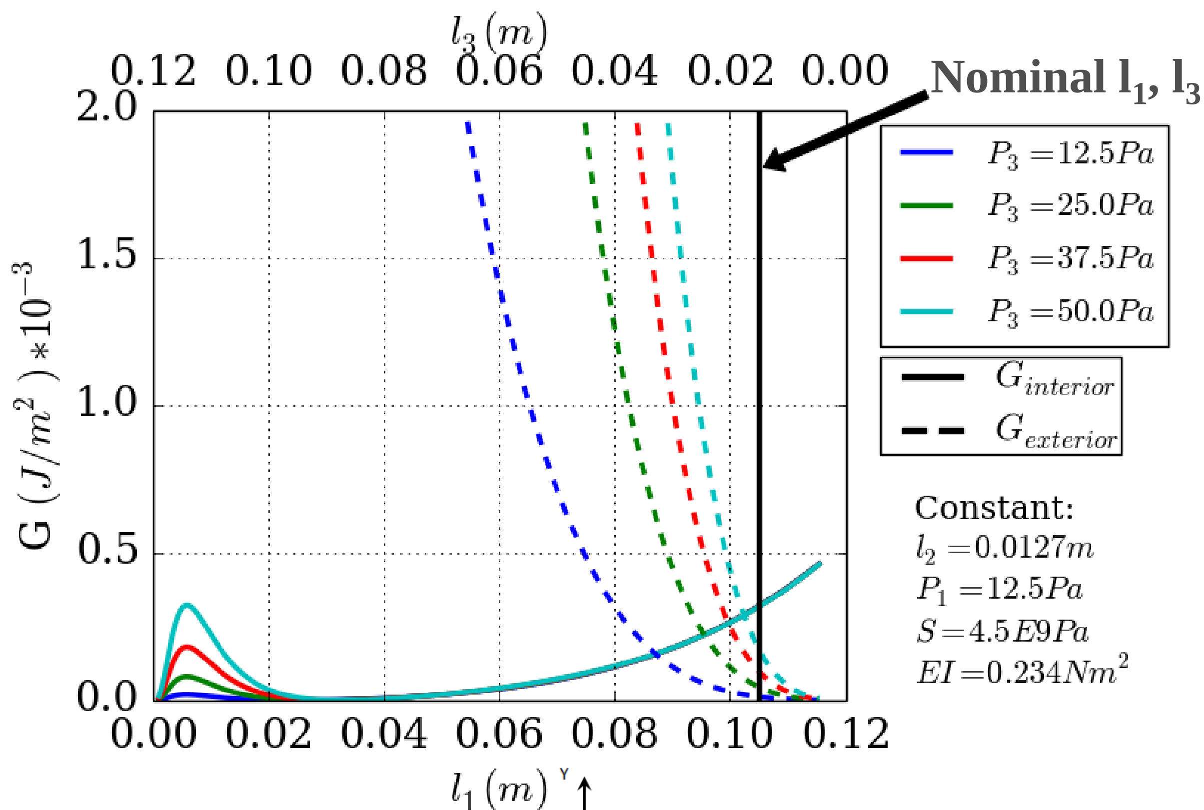

Applied $\mathcal{G}$ at the interior and exterior **edges** of sealant as function of sealant location, ξ, with constant sealant and overall beam lengths. Solid lines represent $\mathcal{G}$ at interior sealant edge and dashed lines represent $\mathcal{G}$ at external sealant edge for different pressures.

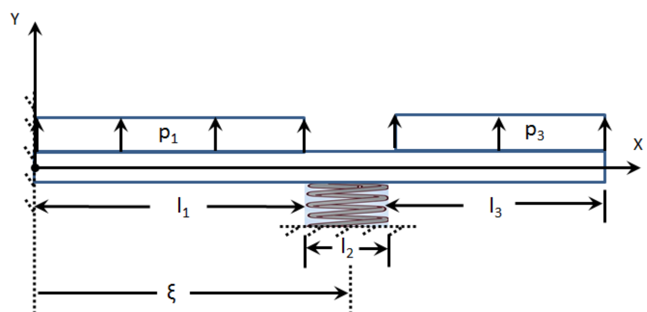

Roofing Shingles

University of South Carolina

Simulations to Assess Potential to Quantify Pressures Using 3D-DIC

σ_w = variability in 3D-DIC measurements = 50µm

σ_{P1} = variability in applied pressure

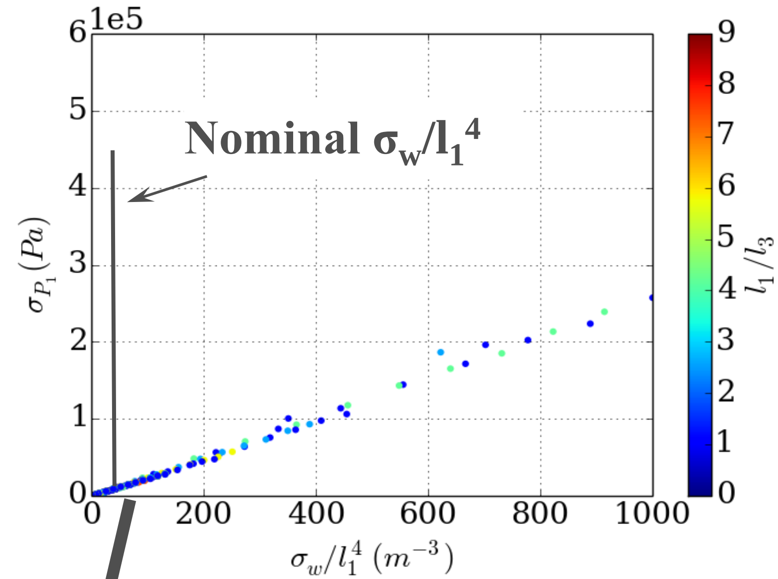

Inset:

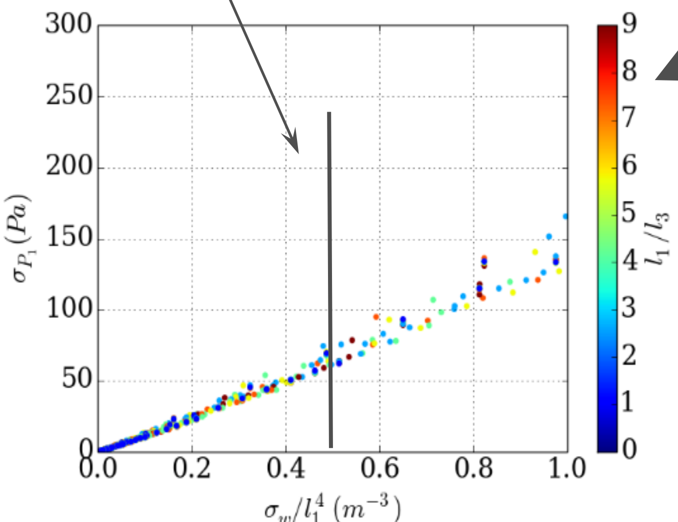

Since P_1 = 12.5Pa, for nominal geometry the standard deviation for a single measurement is nearly 60Pa. Thus, one must take nearly 1800 image pairs to obtain variability of 1.25Pa in the predicted pressure….

Concluding Remarks

- The rapid growth of computer hardware speed since mid-1990s has resulted in both the expansion of computational methods and the explosive growth of digitally-based experimental methods.
- Digital image correlation methods provide a platform for the recording large quantities of full-field deformation data under a broad range of conditions
  - High rate loading (cameras can record images every 5 nanoseconds)
  - High temperature (cameras can acquire usable images for DIC on specimens where T > 1200° C)
  - Small (down to 20μm X 20μm) and large (full-scale aircraft) regions can be measured.
  - Long term studies (experiments lasting several days or longer) have been reported.
- The combination of full-field measurements with theoretical and computational models provides a rich framework for improving our understanding of the physical world.

The Future

"The future of science is neither vague nor unimaginable. It is the result of what we do now."

- Integration with Design and Development
  - Data-driven simulations for design
- Future Trends in Digital Image Based Methods
  - Multiple measurement system integration
  - Continued growth of data-driven parameter estimation approaches
  - Full integration of analysis and measurements for multi-physics studies

University of South Carolina

Integration with Design and Development

Met

A priori information → Current Design → Validation → Assessment → Design Optimization → Final Design

Not Met

- Operational conditions

- **Materials**
  Material parameter identification via
  - *Whole field data*
  - *Novel experiments*

- **Geometry**
  Size and shape validation for component using
  - *Whole field metrology*
  - *Initial specifications*

- Current assembly design, proof or certification test

- Whole field experimental data

- Model/ simulation platform

- Design or test requirement assessment

- Design optimization platform

- TBD

Image correlation based methods provide unique capability to make the measurements required to implement such integrated simulation-measurement design concept

Increments

Integration with Design and Development

- The ability to smoothly integrate full-field measurements using 2D-DIC, 3D-DIC and/or V-DIC with design simulations **requires efficient and robust optimization methodologies** that can effectively identify the constrained optimal combination of
  - Material parameters
  - Structural configurations
  - Operational conditions

- Successful implementation of DIC-based measurement methods with simulation platforms offers **opportunities to replace existing "testing standards"** with a far more robust design methodology

- **Education level** of the next generation of designers **must be adequate** for this approach to be viable.

Future Trends in Digital Image Based Methods

Integration of multiple measurement systems

- ***Synchronized measurements with multiple measurement technologies***
  - CT systems for slow speed events
  - Stereovision systems
    - Slow speed events
    - High speed events
  - Thermographic camera systems
  - Multiple average or local sensor measurements
    - Pressure
    - Loads
    - Moments
    - Voltage
    - Current
    - Other environmental variables
-

University of South Carolina

Acknowledgements

Funding by the following government agencies and the support for our work by the following project directors is gratefully acknowledged

National Science Foundation

Dr. Kenneth Chong

Dr. Oscar Dillon

Dr. Martin Dunn

NASA Langley and HQ

Dr. Charles E. Harris

Dr. Robert S. Piascik

Dr. Stephen W. Smith

Air Force Research Lab

Dr. Scott Fawaz

Dr. James Harter

Dr. Robert Reuter

Army Research Office

Dr. Bruce Lamattina

Dr. Raj. Rajendran

Air Force Office Scientific Research

Dr. Victor Giurgiutiu

Dr. David Stargel

Sandia NL—Albuquerque

Dr. Philip Reu

Dr. Timothy Miller

University of South Carolina

Acknowledgements

Funding by the following government and private organizations and the support for our work by the following project directors is gratefully acknowledged

General Motors Research

Dr. Ching-Shan Cheng

Dr. Pablo Zavattieri

Lockheed Martin

Dr. Glynn Adams

Dr. Edward Ingram

Pechiney Aerospace

Dr. Raphael Muzzolini

Army Research Lab

Dr. Bruce Fink

Boeing Company

Dr. Eui Lim

Acknowledgements

University of South Carolina

- To the graduate students who made this work possible

PhD

Joshua Liu (1984)	Alcoa
Stephen McNeill (1986)	USC Professor
Jounq Min Goan (1988)	GM
P F Luo (1992)	Professor, Taiwan
Gang Han (1993)	Fuji Film
Jin Liu (1997)	Westinghouse
Jeffrey Helm (1999)	Lafayette University
Peng Cheng (2000)	Morgan Stanley
Wenzhong Zhou (2001)	SolidWorks
Hubert Schreier (2003)	Correlated Solutions
Junhui Yan (2004)	Industry
Nicolas Cornille (2005)	Engineer, France
Xiaodan Ke (2007)	Correlated Solutions
Robert James (2008)	Grumman Aerospace
Vikrant Tiwari (2009)	Faculty, IIT New Delhi
Yanqing Wang (2010)	Student (Texas A&M)
Xing Zhao (current)	
Siming Guo (current)	

MS

CC Lee (co-adv, 1983)	Consulting Engineer, DC
Majid Babai (1985)	NASA Huntsville
Jounq Min Goan (1985)	GM
Jinseng Jang (1987)	Electronics industry, Calif.
Hugh Bruck (1988)	Prof, Univ Maryland
Han Gang (1989)	Fuji Film
Timothy Chae (1990)	Oak Ridge Natl Lab
Guang Ma (1991)	Graphics company, Calif
J. Michael Hardin (1991)	Prof, VMI
Jin Liu (1993)	Westinghouse
Ruiyun Wu (1992)	PhD, Notre Dame
Jeffrey Helm (1994)	Prof, Lafayette Univ.
Byron Amstutz (1995)	Anderson Consulting
Jundong Lan (1998)	Consulting engr, Chicago
Michael Boone (2000)	Westinghouse admin
Robert Taylor (2002)	Consulting engineer
John Ward (2004)	GE Gas Turbines
Youzhang Ge (2007)	PhD, RPI
Matthew Hammond (2009)	USAF Aging Aircraft Ctr
Jason Ouzts (2009)	SCANA
Gary Shultis (2010)	CIA
Eileen Miller (2013)	Boeing, Charleston

Future Trends in Digital Image Based Methods

- ***Continued expansion of parameter identification***
  - Common optimization metric;

$$\mathbf{E} = \sum_i \sum_j \left(F(\underline{x}_i, t_j; \mathbf{B}), - f(\underline{x}_i, t_j)\right)^2$$

F() = theoretical function for measurable quantity

f() = experimental measurements for quantity

$\underline{x}_i$ = i^{th} spatial position on specimen

t_j = j^{th} time of interest

B = vector of unknown parameters by minimizing **E**

Examples: mixed mode stress intensity factors using full-field crack tip data, composite material parameters

Future Trends in Digital Image Based Methods

- ***Full integration of analysis and measurements for multi-physics studies***

- Experimental measurements combined with multi-physics models coupling effects from multiple environmental factors.
    - Multi-physics model validation using estimated parameters
    - Model employed for predictions in regimes where experimental measurements are more difficult

"The future? It is impossible to envision the unimaginable, and wonderful to see it happen."

Future Trends in Digital Image Based Methods

University of South Carolina

Recent DIC-Related Activities

- Article in Applied Mechanics Reviews (6/2013)
- Special issue in Experimental Mechanics focusing on Digital Image Correlation (1/2015)
- 2nd edition of book is under development, highlighting the most recent trends in DIC and applications

References

1. Strain Gage Photograph, SGT-1/350-TY11
2. Law, Devries and Wu, Analysis of Drill Stresses by Stress Freezing Photoelasticity, ASME J. Engr. For Industry , 965-970 (1972)
3. Tornari, "Handbook on the Use of Lasers in Conservation and Conservation Science" (2008).
4. http://www.fysikbasen.dk/PrintPopupENG.php?id=92
5. V. J. Parks, "The range of speckle metrology," Exp. Mech. 20, 181-191 (1980).
6. www.ila.de
7. MA Sutton, YJ Chao, and CE Taylor, "Slope Measurements Using Multiplexed Diffraction Gratings as Shearing Components in Shearing Interferometry", Experimental Mechanics, 23 (12) 370-378 (1983).
8. http://www.3ds.com/products/simulia/portfolio/abaqus/abaqus-portfolio/abaqusstandard/
9. http://www.mscsoftware.com/product/msc-nastran
10. J Bystrzycki, J Paszula and RA Varin, Structure and hardness of explosively loaded Fe-Al intermetallic alloys, Materials Science and Engineering: A, 239-240, 546-558 (1997).
11. Prof. William Fourney, University of Maryland, personal communication
12. JD Helm, MA Sutton and ML Boone, "Characterizing Crack Growth in Thin Aluminum Panels Under Tension-Torsion Loading with Three-Dimensional Digital Image Correlation", Nontraditional Methods of Sensing Stress, Strain and Damage in Materials and Structures, ASTM STP 1323 3-14 (2001).
13. Zhigang Wei, Xiaomin Deng, Michael A. Sutton, Junhui Yan, C.-S. Cheng Pablo Zavattieri, "Modeling of mixed-mode crack growth in ductile thin sheets under combined in-plane and out-of-plane loading", Engineering Fracture Mechanics, 78 (17), 3082-3101 (2011).
14. P Majumdar, X-Radia Micro-CT image, personal communication .
15. TC Chu, WF Ranson, MA Sutton, WH Peters, III, "Application of Digital Image Correlation Techniques to Experimental Mechanics", Experimental Mechanics, 25 (3) 232-245 (1985).
16. JD Helm, personal communication.
17. P. Pollock, L. Yu, M.A. Sutton, S. Guo, P. Majumdar, and M. Gresil,."Full-Field Measurements for Determining Orthotropic Elastic Parameters of Woven Glass-Epoxy Composites Using Off-Axis Tensile Specimens", Experimental Techniques (in press).
18. J. Liu, MA Sutton and JS Lyons, "Experimental Characterization of Crack Tip Deformations in Alloy 718 at High Temperatures", ASME Journal of Engineering Materials and Technology, 20 (1) 71-78 (1998).
19. JS Lyons, J Liu, and MA Sutton, "High Temperature Deformation Measurements Using Digital Image Correlation", Experimental Mechanics., 36 (1) 64-71 (1996).

References

University of South Carolina

20. MA Sutton, W Zhao, SR McNeill, JD Helm, WT Riddell and RS Piascik, "Local Crack Closure Measurements: Development and Application of a Measurement System Using Computer Vision and a Far-Field Microscope", to be published in ASTM STP 1343 on Crack Closure Measurements, K. Smith and J. McDowell, Ed, 145-156 (1999)
21. WT Riddell, RS Piascik, MA Sutton, W. Zhao, SR McNeill and JD Helm, "Local Crack Closure Measurements: Determination of Fatigue Crack Opening Loads from Near-Crack-Tip Measurements", to be published in ASTM STP 1343 on Crack Closure Measurements, K. Smith and J. McDowell, Ed 157-174 (1999).
22. HW Schreier, D Garcia and MA Sutton, "Advances in Stereo Light Microscopy", Experimental Mechanics, 44 (3) 278-289 (2004).
23. MA Sutton, N. Li, DC Joy, AP Reynolds and XD Li, "Scanning Electron Microscopy for Quantitative Small and Large Deformation Measurements; Part I. SEM Imaging at Magnification from 200 to 10,000", Experimental Mechanics 47 (6) 775-788 (2007).
24. MA Sutton, N. Li, D. Garcia, N. Cornille, J. Orteu, S. McNeil, H. Schreier, X. D. Li , A. P. Reynolds, "Scanning Electron Microscopy for Quantitative Small and Large Deformation Measurements; Part II: Experimental Validation for Magnifications from 200 to 10000", Experimental Mechanics, 47 (6) 789-804 (2007).
25. WA Scrivens, Y Luo, MA Sutton, SA Collette, ML Myrick, P Miney, PE Colavita, AP Reynolds and X-D Li, "Development of Patterns for Digital Image Correlation Measurements at Reduced Length Scales", Experimental Mechanics 47 (1) 63-79 (2007).
26. X. Li, H. Gao, WA Scrivens, D Fei, X Xu, MA Sutton, AP Reynolds, and ML Myrick, "Nano-mechanical characterization of single-walled carbon nanotube reinforced epoxy composites", Nanotechnology 7 1-9 (2007).
27. X-D Li, W-J Xu, MA Sutton, and M Mello, "In situ nanoscale in-plane deformation studies of ultrathin polymeric films during tensile deformation using atomic force microscopy and digital image correlation techniques", Nanotechnology, 16 (1) 4-13 2007.
28. MA Sutton, Ning Li, D Garcia, N Cornille, JJ Orteu, SR McNeill, HW Schreier and X Li. "Metrology in a scanning electron microscope: theoretical developments and experimental validation, Measurement Science and Technology, 17 2613-2622 (2006)
29. ZH Xu, XD Li MA Sutton and N Li, "Drift and spatial distortion elimination in atomic force microscopy images by the digital image correlation technique", Journal of Strain Analysis for Engineering Design, 43 729-743 (2008).
30. T. Zhu, MA Sutton, N Li, X-D Li and A.P. Reynolds, "Quantitative Stereovision in a Scanning Electron Microscope", Experimental Mechanics, 51 (1) 97-109 (2011).

References

31. ZH Xu, H Jin, WY Lu, MA Sutton and XD Li, Influence of Scanning Rotation on Nanoscale Artificial Strain in Open Loop AFM", Experimental Mechanics, 51 (4), 619-624 (2011).
32. JD Helm, SR McNeill and MA Sutton, "Improved 3-D Image Correlation for Surface Displacement Measurement", Optical Engineering, , 35 (7) 1911-1920 (1996).
33. JD Helm, MA Sutton and SR McNeill, "Deformations in wide, center-notched, thin panels: Part I: Three dimensional shape and deformation measurements by computer vision", Optical Engineering, 42 (5) 1293-1305 (2003)
34. JD Helm, MA Sutton and SR McNeill, "Deformations in wide, center-notched, thin panels: Part II: Finite element analysis and comparison to experimental measurements", Optical Engineering, 42 (5) 1306-1320 (2003).
35. http://www.yxlon.com/Products/CT-system
36. MA Sutton, JJ Orteu and HW Schreier, "Image Correlation for Shape, Motion and Deformation Measurements", ISBN 978-0-387-78746-6, Springer (2009).
37. ZG Wei, XM Deng, MA Sutton, JH Yan, CS Cheng and P Zavattieri, "Modeling of mixed-mode crack growth in ductile thin sheets under combined in-plane and out-of-plane loading", Engineering Fracture Mechanics, 78 (17), 3082-3101 (2011).
38. Y-N Li, T. Wierzbicki, MA Sutton, J-H Yan and X-M Deng, "Mixed Mode Stable Tearing of Thin Sheet Al 2024 Specimens: Experimental Measurements and Finite Element Simulations Using a Modified Mohr-Coulomb Fracture Criterion", Intl J. Fracture, 168 (1) 53-71 (2011).\
39. JH Yan, MA Sutton, X. Deng and C-S Cheng, "Mixed-mode fracture of ductile thin sheet materials under combined in-plane and out-of-plane loading", Intl Journal of Fracture, 144 297-321 (2007)
40. MA Sutton, JD Helm and ML Boone, "Experimental Study of Crack Growth in Thin Sheet Material under Tension-Torsion Loading", International Journal of Fracture 109 285-301 (2001).MA Sutton, J Yan, X Deng, C-S Cheng* and P Zavattieri, "3D Digital Image Correlation to Quantify Deformation and COD in Ductile Aluminum Under Mixed-mode I/III Loading", Optical Engineering 46(5) 051003-1 to 051003-17 (2007).
41. TK Borg, JL Stewart and MA Sutton, Seeing is Believing: Imaging the Cardiovascular System", Microscopy and Microanalysis, 11(3):189-199 (2005).
42. MA Sutton, XD Ke, SM Lessner, M Goldbach, M Yost, F Zhao, HW Schreier, "Strain Field Measurements on Mouse Carotid Arteries Using Microscopic Three-Dimensional Digital Image Correlation," J. Biomed. Matl. Res. 84A 178-190 (2007).
43. X. Ke, M.A. Sutton, S. Lessner and H.W. Schreier, Robust stereovision and calibration methodology for accurate 3D digital image correlation measurements on submerged objects, Journal of Strain Analysis for Engineering Design 43 689-704 (2008).

University of South Carolina

References

44. JF Ning, VG Braxton, Y Wang, MA Sutton, YQ Wang and SM Lessner, “Speckle Patterning of Soft Tissues for Strain Field Measurement Using Digital Image Correlation: Preliminary Quality Assessment of Patterns”, Microscopy and Microanalysis, doi:10.1017/S1431927610094377 (2011).
45. P Badel, S Avril, SM Lessner, MA Sutton. “Mechanical identification of layer-specific properties of mouse carotid arteries using 3D-DIC and a hyperelastic anisotropic constitutive model”, Computer Methods in Biomechanics and Biomedical Engineering, 15 (1) 37-48 (2011).
46. Y Wang, J-F Ning, MA Sutton and SM Lessner, “Development of a quantitative mechanical test of atherosclerotic plaque stability”, Journal of Biomechanics 44(13):2439-45 (2011).
47. Y Wang, SM Lessner, A Fulp, JA Johnson and MA Sutton, “Adhesive Strength of Atherosclerotic Plaque in a Mouse Model Depends on Local Collagen Content”, Journal of Biomechanics (in press).
48. JF Ning, SW Xu, Y Wang, SM Lessner, MA Sutton, K Anderson and JE Bischoff, “Mouse carotid artery studies: deformation measurements and material property estimation using microstructure-based constitutive model”, Journal of Biomechanical Engineering 132 121010-121023 (2011).
49. Y-Q Wang, MA Sutton, X-D Ke and HW Schreier, “Error Propagation in Stereo Vision: Part I: Theoretical Developments”, Experimental Mechanics 51 (4) 405-422 (2011).
50. X-D Ke, HW Schreier, MA Sutton and Y-Q Wang, “Error Propagation in Stereo Vision: Part II: Experimental Validation”, Experimental Mechanics, 51 (4), 423-441 (2011).
51. YQ Wang, MA Sutton and HW Schreier, Quantitative Error Assessment in Pattern Matching: Effects of Intensity Pattern Noise, Interpolation, Subset Size and Image Contrast on Motion Measurements, Journal of Strain, 45 160-178 (2009).
52. HS Zhang, X Zhao, XM Deng , MA Sutton, AP Reynolds, SR McNeill, “Investigation of Material Flow during Friction Extrusion Process”, Journal of Material Processes (in review).
53. http://www.norplex-micarta.com/
54. S-M Guo M.A. Sutton, P. Majumdar, K.M. Reifsnider, Lucy Yu and M. Gresil, “Development and Application of an Experimental System for the Study of Thin Composites Undergoing Large Deformations in Combined Bending-Compression Loading”, Journal of Composite Materials (in press).
55. SM Guo, M Gresil, MA Sutton, XM Deng, KW Reifsnider and P Majumdar, Nonlinear Predictive Model for Combined Bending-Compression Loading of an Orthogonal Plane Weave Composite Laminate Structure, J. Composite Materials (in review).
56. X Zhao, V Tiwari, MA Sutton, X Deng, WL Fourney and U Leiste, “Scaling of the Deformation Histories for Clamped Circular Plates Subjected to Buried Charges”, Intl Journal of Impact Engineering (in press).

University of South Carolina

References

57. V Tiwari, MA Sutton, S.R. McNeill a, Shaowen Xu a, Xiaomin Deng, D Bretall, WF Fourney, Application of 3D image correlation for full-field transient plate deformation measurements during blast loading, Intl J. Impact Engr, 36 862-874 (2009).
58. X. Zhao, WF Fourney, MA Sutton, X Deng and U. Leiste, “Experimental Investigations on Mitigating Acceleration of Vehicle Structures Impacted by Explosive Detonation” Parts I and II, Experimental Mechanics (in review)
59. MA Sutton, V Tiwari, WL Fourney, SR McNeill, S-W Xu, X-M Deng, J-H Yan, X. Zhao and D Bretall. “Full-field deformation measurements under explosive loading conditions using multi-image pattern analysis”, Fragblast,. 10 (1), 1-21 (2011).
60. S-W Xu, X-M Deng, V. Tiwari and MA Sutton, “An Inverse Analysis Approach for Pressure Load Identification”, Intl J. Impact Engr. 37 (7) 865-877 (2010).
61. S-W Xu, X-M Deng, V. Tiwari and MA Sutton, “Identification of Interaction Pressure Between Structure and Explosive with Inverse Approach”, Experimental Mechanics, DOI: 10.1007/s11340-010-9390-y.

Brief History: Measurement Methods

- Issues associated with extraction of deformation information using film as a recording media
  - Non-linearity in film
  - Film processing *(darkroom)*
  - Film stability and handling
  - Laser illumination
  - De-correlation effects *(previous slide)*
  - Exorbitant time requirements
  - Inaccuracies in reconstruction process
    - fringe location
    - film expansion/contraction
    - relationship of object to image coordinates
    - distortions in imaging process

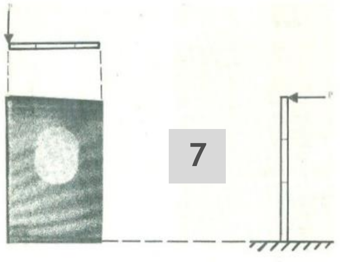

University of South Carolina